$UBVRI$ Photometry of the Type Ic SN 1994I in M51

Michael W. Richmond
Department of Astrophysical Sciences, Princeton University, Princeton NJ 08544
Electronic mail: richmond@astro.princeton.edu

Schuyler D. Van Dyk, Wynn Ho, Chien Peng, Young Paik, Richard R. Treffers,
Alexei V. Filippenko[1]
Astronomy Department, University of California, Berkeley CA 94720

Javier Bustamante-Donas
Dept. of Ethics and Sociology, Universidad Complutense de Madrid, Madrid 28040, Spain

Michael Moeller and Claus Pawellek
Luebeck Public Observatory, Luebeck, Germany

Heather Tartara and Melody Spence
Oil City High School, Oil City, PA 16301

ABSTRACT

We present optical photometry for the type Ic SN 1994I in M51 (NGC 5194) from UT March 31 to Aug 6, 1994, starting eight days before B-band maximum and ending three months later. We estimate the extinction to SN 1994I was considerable and quite uncertain, $A_V = 1.4 \pm 0.5$ mag, making a detailed comparison to other supernovae difficult. Using a distance modulus $\mu = 29.6 \pm 0.3$ mag to M51, we calculate absolute magnitudes and a quasi-bolometric light curve for the supernova. It appears that SN 1994I was less luminous than "normal" type Ia SNe. There is strong evidence that the ejecta of SN 1994I were much less massive than those of other SNe.

1. Introduction

SN 1994I in the face-on Sc galaxy M51 (NGC 5194, "The Whirlpool") was discovered on UT April 2, 1994, independently by at least four sets of observers: Tim Puckett and Jerry Armstrong, Wayne Johnson and Doug Millar, Richard Berry, and Reiki Kushida (Puckett *et al.* 1994). Its spectrum caused some confusion in the first few days after discovery, being interpreted as similar to that of a type II (Schmidt & Kirshner 1994a), type Ib (Filippenko, Matheson, & Barth 1994), type Ic (Schmidt, Challis, & Kirshner 1994), and peculiar type Ia (Turatto & Zanin 1994); after

---

[1] Also associated with the Center for Particle Astrophysics, University of California at Berkeley

a week, however, a consensus grew that it was a type Ic event (Clocchiatti *et al.* 1994; Kirshner *et al.* 1994). Detailed spectroscopic studies by Wheeler *et al.* (1994) and Filippenko *et al.* (1995) confirmed this classification, which is largely the end of a process of elimination: type Ic SNe show no lines of hydrogen (hence are not type II), lack the deep Si II absorption trough near 6150 Å (hence are not type Ia), and also lack absorption lines of He in the optical (hence are not type Ib). Note, however, that Filippenko *et al.* did detect the He I λ 10830 line in SN 1994I, showing that at least a small amount of helium must have been present in its atmosphere.

The position of the SN is slightly uncertain: Rupen *et al.* (1994) used the VLA to measure a radio position $\alpha = 13^{\mathrm{h}}27^{\mathrm{m}}47\overset{\mathrm{s}}{.}731$, $\delta = +47^{\circ}26'57\overset{''}{.}84$, equinox 1950.0, corresponding to a position in the J2000.0 system of $\alpha = 13^{\mathrm{h}}29^{\mathrm{m}}54\overset{\mathrm{s}}{.}06$, $\delta = +47^{\circ}11'29\overset{''}{.}96$. Morrison & Argyle (1994) report that optical measurements with a meridian circle yield $\alpha = 13^{\mathrm{h}}29^{\mathrm{m}}54\overset{\mathrm{s}}{.}072$, $\delta = +47^{\circ}11'30\overset{''}{.}50$, equinox J2000.0. The small difference may be due to the strong gradient in light from the nucleus of M51 at the position of the supernova, as Morrison and Argyle state.

We initiated a program of multicolor photometry at Leuschner and Lick Observatories, and report here our results. In addition, we have collected several very early images taken at other sites and reduced them in the same manner as our own.

Section 2 contains a description of the observations. Section 3 discusses the "template subtraction" method of photometry we used to extract the light of SN 1994I from its environs in the disk of M51. Our calibration of the measurements onto the standard Johnson-Cousins system appears in Section 4. In Section 5 we present light curves of SN 1994I. Since this event occurred close to the nucleus of M51, it is not surprising that there are several indications of a large amount of extinction, which we describe in Section 6. In Section 7, we discuss the distance to M51, and calculate absolute magnitudes in all passbands for our adopted extinction. In addition, we calculate a quasi-bolometric light curve by summing the observed optical fluxes. In Section 8, we compare the light curves of SN 1994I with those of the type Ic SN 1987M. We place our conclusions in Section 9. An Appendix lists details of the equations used to place our observations onto the standard Johnson-Cousins photometric system.

2. Observations

Figure 1 shows SN 1994I, its host galaxy M51, and reference stars A, B, C, and D. We report on observations obtained mainly by the two telescopes at Leuschner Observatory and one at Lick Observatory, with several very early observations from telescopes at other sites. All data were measured from CCD images, and reduced to a common magnitude sequence of comparison stars.

At Leuschner Observatory, we used a 50-cm and a 76-cm telescope, both reflectors equipped with CCD cameras (Richmond, Treffers, & Filippenko 1993; Richmond *et al.* 1994, henceforth R94). The full-width at half-maximum (FWHM) of stellar images was usually $3'' - 4''$. Our exposure times varied from about 200 seconds (in the R and I bands) to 1500 seconds (in the U and, at late time, B bands). We created bias frames by taking the median of five images each afternoon, and flatfield frames from the median of five exposures of the twilight sky; we then applied them to the raw images in the usual fashion.

Lick Observatory's 1-m Nickel telescope is equipped with a 2048×2048-pixel CCD camera, which we operated in 2×2 binned mode, yielding a plate scale of $0\overset{''}{.}37$ per pixel. The seeing was typically $2 - 3''$ FWHM, and exposure times ranged from 60 to 1080 seconds. The frames were corrected for bias and flatfield as described above.

We have images at very early times from two additional sources. One of us (JBD) used a 20-cm Schmidt-Cassegrain telescope and an SBIG ST-4 CCD camera without filters to obtain exposures of 160 and 180 seconds on Apr 2 UT. The plate scale is $3\overset{''}{.}7 \pm 0\overset{''}{.}2$ per pixel, and stellar images appear to have FWHM about 1.5 pixels. Comparing the raw, instrumental differences in magnitude between stars A, B, C, and D with those listed in Table 1, we find the response of this system to be closest to the Cousins R band. Specifically, we find instrumental differences $(B - A) = 1.32$, $(C - A) = 1.73$, and $(D - A) = 1.49$. Defining r to be the magnitude of a star in the instrumental system, we can write $R = r + k_r(V - R) + C$, where C is an arbitrary zero-point offset. We can find a value for k_r using the instrumental magnitudes and our adopted V and R magnitudes for the comparison stars listed in Table 1. We find $k_r = -0.41 \pm 0.25$. We will designate these data "R."

MM and CP used a 49-cm f/4.2 telescope at the Luebeck Public Observatory in Germany, equipped with an SBIG ST-6 CCD camera and no filter, to acquire three images of SN 1994I on March 31 UT. The scale is $2\overset{''}{.}6$ per pixel. All objects show trails of about 4 pixels in the North-South direction, and a width of about 1.5 pixels. The exposure times were 10, 15 and 10 seconds. Although a correction was made for dark count, no flat-fielding was applied to the images. Once again using the instrumental magnitude differences between stars A, B, C, and D, we find these images to have a response closest to the Johnson-Cousins V band. In this case, the instrumental differences are $(B - A) = 1.76$, $(C - A) = 1.72$, and $(D - A) = 1.77$. Asserting that $V = v + k_v(V - R) + C$, we calculate $k_v = -0.26 \pm 0.42$. We will use the term "V" when referring to these data.

3. Extracting instrumental magnitudes

Light from SN 1994I was surrounded by light from the galaxy's nucleus, making photometry a difficult task. In order to extract instrumental magnitudes from each image, we attempted to use the "rotsub" technique described in Richmond et al. (1995; henceforth R95), but found that the strong spiral features of M51 led to significant residuals at the position of the SN (however, we did use measurements of the comparison stars derived by this procedure; see Section 4 below). Therefore, we turned to the "tempsub" method, also described in R95 and summarized briefly here. After the SN had faded from visibility, we acquired images of M51 in good seeing (FWHM

$\approx 1\farcs6$) with the Nickel 1-m telescope at Lick Observatory, one each in $BVRI$. We used a set of IRAF[2] tools to stretch and rotate these "template" images to match each image taken while the SN was visible, convolved them with a Gaussian to equalize the seeing disks, scaled them to match the sky-subtracted intensity of star A in a circular aperture of radius 10 pixels, and then subtracted the "template" from the original. This procedure yielded images in which SN 1994I stood out clearly from its surroundings, as Figure 2 shows; the results were cleaner than those produced by other techniques we tried. We then measured the light of star A (in the convolved template image) and the SN (in the subtracted image), using identical synthetic circular apertures of radius 0.75 times the FWHM of the convolved template image, and identical sky annuli. The sky value calculated for the SN in the subtracted image was very close to zero.

In order to gauge the accuracy of the subtraction, we used the DAOPHOT2 package in IRAF to add artificial stars to the raw images. We used star A to define a point-spread function (PSF) for each image, and added into the image four copies of the PSF scaled to match the brightness of the SN; we placed the copies symmetrically around the nucleus of M51, at roughly the same distance as SN 1994I. After performing the template subtraction, we measured the brightness of each artificial star and calculated the standard deviation from the mean of the four values. We used this as an estimator of the uncertainty in the instrumental magnitude of SN 1994I. Propagating the magnitudes through our photometric solution yielded the final uncertainties we list in Tables 4 and 5.

The U-band data, however, must be treated differently. Our instrument is so insensitive to light in this passband that even very long exposures yielded very weak signals from the SN, star A, and the nucleus of M51; no other sources were visible. The "tempsub" technique mentioned above involves subtracting a model from the original image, and then measuring the remaining light. For the U-band, in which the signal-to-noise ratio for both the SN and the comparison star A is very low, such a procedure will increase the noise and degrade the signal even further. We chose to perform pure aperture photometry on each original U-band image, using a circular aperture of radius $r = 3$ pixels $= 1\farcs86$. Light from the nucleus of M51 was so feebly detected that it barely reached the position of SN 1994I, alleviating the background subtraction that posed such a problem in $BVRI$. The small amount of "sky" that we detected was estimated from an annulus with inner radius $5\farcs0$ and outer radius $11\farcs2$. We adopt the uncertainties calculated by the IRAF task qphot, which are based on photon and readout noise, and propagate them through the photometric solution.

4. Calibration

[2]IRAF is distributed by the National Optical Astronomy Observatories, which are operated by the Association of Universities for Research in Astronomy, Inc., under contract to the National Science Foundation.

We have adopted star A (see Figure 1) as our primary comparison star; the fainter stars B, C and D provide checks on the lack of variation of star A, and yield estimates of the precision of photometry. Soon after SN 1994I was discovered, Harold Corwin (1994) distributed his measurements of stars in the field of M51, which were the source of several magnitudes listed on the Thompson-Bryan (1989) chart for the galaxy. Corwin's message warned that background subtraction was difficult for those stars immersed in the galaxy's light, and that his values should be used only for preliminary reduction of SN photometry. Nonetheless, his values were very useful to us and others, in the first few months after discovery, and we list them in Table 1. On 1995 April 24 UT, we used the 1-m Nickel telescope at Lick Observatory to observe the field of SN 1994I and five multi-star fields from the list of Landolt (1992) in $BVRI$. Using the photcal task in IRAF, we calculated a photometric solution for each passband of the form

$$V = v + v1 + v2 * X + v3 * (b - v) + v4 * X * (b - v)$$

where V denotes a standard magnitude, b and v instrumental values, and X the airmass. We list the solutions and their formal uncertainties in the Appendix. Using the solutions, we were able to calculate magnitudes on the standard system for comparison stars A, B, C, and D, which we list in Table 1. We adopt the Lick calibration for star A as the basis for all $BVRI$ photometry in this paper, since we believe CCD photometry allows more accurate subtraction of the complicated background near star A than does aperture photometry. Since we were unable to acquire U-band observations at Lick, however, we maintain the U-band magnitude of star A provided by Corwin.

Having adopted a set of magnitudes for the comparison stars, we were able to transform all raw magnitudes onto the Johnson-Cousins system. The Lick Observatory data were corrected using the color transformation coefficients described above. Leuschner Observatory data were placed onto the standard system using color transformation coefficients listed in the Appendix, again using the Lick observations of star A to provide a zero-point. The size of the corrections was typically less than 0.1 mag.

The very earliest data, listed in Table 2, for which only a single passband was observed each night, are not corrected for any color effects. How large an error could this cause? The error ϵ depends on the difference between the colors of our comparison star A and the SN, and on the color term of the detector; for example, in the R band,

$$\epsilon = k_r((V - R)_A - (V - R)_{SN}) = k_r \Delta(V - R),$$

where k_r corrects instrumental r magnitudes into the standard system, based on the standard $(V - R)$ color. Table 1 shows that star A has $(V - R) = 0.36$. The earliest Leuschner observations of SN 1994I show $(V - R) \approx 0.25$, but the color might have been bluer at earlier times. If we assume that the SN radiated like a blackbody in the first few days after it exploded, and assume it had a temperature $T = 20,000$ K, we find $(V - R) = -0.01$, in which case the difference in color between the SN and star A would have been $\Delta(V - R) = 0.37$. Let us now consider each of the three single-bandpass detections in turn. The March 31.43 V-band point from the

Leuschner 76-cm telescope is subject to $k_v = 0.02 \pm 0.01$; in the worst case, $k_v = 0.03$, the color term would introduce an error of $\epsilon = 0.01$ mag, negligible when compared to the internal error in extracting the magnitude of the SN. The March 31.96 "V"-band point from Luebeck could suffer from $k_v = -0.26 \pm 0.42$; in the worst case, if $k_v = -0.68$, the color term could be $\epsilon = 0.25$ mag. Since the internal error of the magnitude extracted from the three Luebeck images is 0.40 mag, this contributes a small amount to the overall uncertainty listed in Table 2. Finally, the early observations by JBD have a color term $k_v = -0.41 \pm 0.25$; in the worst case, the color term $k_v = -0.66$ could introduce an error of 0.24 mag, larger than the internal scatter of 0.08 mag measured from the extraction process. Since we have pushed all effects to their extremes in these calculations, we believe the tabulated uncertainties to be conservative ones.

We can check that star A did not vary over the course of our observations by comparing it to the other three bright stars in the field. These check stars can also be used to derive limits to the precision of our photometry. In the discussion below, we use raw magnitudes extracted from the frames processed via the "rotsub" procedure, since the residuals at positions of stars left by template subtraction are difficult to interpret. No difference between star A and any other star showed a significant linear trend over the 75-day period 1994 March 28 - June 11; the values of $(A - B)$ yield the most stringent limits, permitting a change in the mean of no more than $0.08, 0.01, 0.005, 0.006$ mag over that period in B, V, R, I, respectively. We list the internal precision of raw differential magnitudes in Table 3, to provide a feeling for the precision of photometry from our images. All of the comparison stars are located in much cleaner environments than SN 1994I, farther from the nucleus; hence, their photometry is somewhat more precise than that of the supernova. The values in Table 3 are therefore lower bounds on the uncertainty in measurements of the SN, at times when it had comparable apparent magnitude.

5. Optical Light Curves

In Figure 3 we present the $UBVRI$ light curves in a single graph, and in Figures 5-9 each passband separately. Tables 4, 5, and 6 contain the data from the Leuschner 50-cm, 76-cm, and Lick telescopes, respectively. In Table 2 we place the early data gathered by all telescopes. Before we discuss the light curves, let us calculate the times and values of the peak apparent brightness, so that we can use the time of B-band maximum as a fiducial point.

The times and magnitudes of the peak in each band are listed in Table 7. To determine these values, we fit polynomials of increasing order to the points on each light curve between JD 2,449,444 and 2,449,458. We increased the order of the polynomial until the resulting value of χ^2 stopped decreasing significantly (the highest-order fit being quintic). The peak of the fitted polynomial is listed in Table 7. To determine the uncertainties in these fits, we changed each polynomial coefficient until the value of χ^2 of the fit increased by one; we adopted the maximum resulting difference in peak magnitude or time as the uncertainty in the fitted value. Note that we added U-band data from the preliminary analysis of Schmidt & Kirshner (1994b; referred to as

"CfA" in Tables and Figures) to our 4 U-band points in order to make a decent fit; in all other passbands, we fit Leuschner and Lick data only.

The final row in Table 7 lists the Δm_{15} parameter for each passband except U, which lacks sufficient data. Following Phillips (1993), we define Δm_{15} in passband X as the difference between the peak magnitude in X, and the magnitude 15 days after that peak. Since all our light curves have a gap at the crucial period, we were forced to interpolate. We fit polynomials to the set of data between 10 and 20 days after peak, and found that a parabola accounted well for the slight inflection point in the light curves at this time. We added in quadrature the uncertainty in the peak magnitude and this interpolated value to calculate the uncertainty in Δm_{15}. Note that all values of Δm_{15} are larger than those of "normal" type Ia supernovae; for example, SN 1994I had $\Delta m_{15}(B) = 2.07 \pm 0.03$ mag, and $\Delta m_{15}(I) = 1.08 \pm 0.02$ mag, whereas R95 shows that SN 1994D had $\Delta m_{15}(B) = 1.31 \pm 0.08$ mag, and $\Delta m_{15}(I) = 0.71 \pm 0.05$ mag.

How well do our light curves agree with others in the literature? Together with our own measurements, we plot in Figure 4 the data of Schmidt & Kirshner (1994b), from a preliminary analysis which was distributed by E-mail in mid-May 1994. A number of early theoretical papers (such as Iwamoto *et al.* 1994) were based on this set of data. In general, we find very close agreement between the Schmidt & Kirshner points and our own. Other published light curves, by Yokoo *et al.* (1994) and Lee *et al.* (1995), agree with ours at early times, but deviate increasingly as the SN becomes fainter; as Figure 4 shows, they find the SN to be brighter than we do. Since their telescopes and sites were comparable to ours, we believe the differences are due to the different methods by which each group extracted instrumental magnitudes from its images. When a faint object is surrounded by a bright background, improper subtraction of the background nearly always yields measurements in which the object appears *brighter* than it actually is. Our "tempsub" technique does a better job of removing the contribution of light from the nucleus of M51 than either PSF-fitting (Lee *et al.*) or surface-fitting (Yokoo *et al.*).

Let us consider the light curves in each bandpass (see Figures 5-9). The U-band light curve (Figure 5) is very sketchy, and one can say little more than it declined very quickly after maximum light. As R95 mentioned, Leuschner Observatory U-band observations can show large (up to ~ 0.5 mag) deviations from the standard Johnson-Cousins system; in the present case, the agreement with the CfA data (and with that of Lee *et al.* 1994) suggests that our calibration was more successful than it was for SN 1994D.

The B-band light curve, shown in Figure 6, rises and falls quickly, reaching an inflection point sometime around fifteen days after maximum and eventually settling into linear decline. Fitting a straight line to the data after JD 2,449,500, we find a slope of 0.017 magnitudes per day, albeit with substantial uncertainty. There is some evidence for flattening of the light curve at late times.

Several early detections define clearly the very steep rise to maximum in the V-band, shown in Figure 7. The SN must have risen at least 2.4 mag in the 2 days between the upper limit on March 29 and the first measurement, and another 0.9 mag within the next 12 hours. The time from the first V-band detection to V-band peak light is about 9 days. As in the B-band, the light curve falls steeply after maximum, then reaches a linear decline at late times, at a rate of 0.021 mag per day. The last two points indicate that the light curve flattened significantly at the end of our observations.

In Figure 8, one sees another very sharp rise to maximum light. Our early R-band observations constrain the SN to have brightened by over 4 magnitudes in about 5 days before being detected. About 8 days elapsed from the first detection in R-band to maximum light in R. The peak of the light curve is somewhat broader than those in B and V, but the late-time decline rate similar: 0.017 mag per day. As in the V-band, the last two points indicate a flattening of the light curve.

The I-band light curve, shown in Figure 9, exhibits the widest peak and weakest "knee" separating the post-maximum fall from the late-time decline. Again using data after JD 2,449,500, we find a linear slope of 0.021 mag per day. The final two points are substantially brighter than the extrapolated curve.

We next construct color curves for SN 1994I, and plot them in Figures 10 to 13. In each figure, the color rapidly reddens from discovery to roughly JD 2,449,465; after that time, the $(B - V)$ and $(V - R)$ values turn back to the blue. This turning point occurs at the same time as the "knee" in the B and V light curves. Both features probably occur as the ionization front, or pseudo-photosphere, of the supernova reaches into the core of the ejecta and the SN makes the transition from being optically thick to optically thin. The $(R - I)$ color continues to redden for several more weeks, reaching what might be a plateau at $(R - I) \approx 0.7$ mag at the end of our observations.

Note that the earliest measured colors of SN 1994I are considerably redder than is typical for most SNe. The first $(B - V)$ datum, for example, is 0.38 mag. According to Filippenko *et al.* (1995), the spectrum at this time was a relatively smooth and featureless continuum, suggesting that the SN's atmosphere was hot — hot enough, perhaps, to resemble a blackbody. Using the Bessell (1979) flux/magnitude relationships, we find that $(B - V) = 0.38$ mag corresponds to a blackbody of temperature $T = 7950$ K; but such a cool atmosphere should also produce more lines than were seen in the earliest spectrum. Hotter blackbodies yield bluer colors: $T = 15,000$ K corresponds to $(B - V) = 0.00$ mag, and $T = 20,000$ K corresponds to $(B - V) = -0.09$ mag. If one postulates that SN 1994I resembled a perfect blackbody in the first days after discovery, then its observed colors suggest a moderate amount of reddening.

The colors at maximum remain redder than those of some types of SNe. As Figure 11 shows, at the time of maximum light in B, JD 24499450, $(B - V) \approx 0.8$ mag. Even after correcting for extinction of $E(B - V) = 0.45$ mag (see Section 6), the intrinsic color of SN 1994I was $(B - V)^0 \sim 0.35$. The "normal" type Ia SNe, such as SNe 1980N (Hamuy *et al.* 1991) and 1994D (Richmond *et al.* 1995), show $(B - V) \approx 0.0$. The newly-recognized class of "subluminous" SNe Ia, such as SNe 1991bg (Filippenko *et al.* 1992; Leibundgut *et al.* 1993) and 1992K (Hamuy *et al.* 1994), are even more red than SN 1994I, with SN 1991bg reaching $(B - V)^0 \sim 0.7$ at maximum.

Each of the $BVRI$ light curves exhibits a linear decline of about 0.020 magnitude per day (and becoming less steep at the end our observations), corresponding to an exponential decrease in luminosity. The radioactive decay of ^{56}Co yields a smaller slope, 0.0098 mag per day. Therefore, if the late-time light curve of SN 1994I is powered by ^{56}Co, a substantial fraction of the high-energy photons must escape directly from the ejecta, rather than interacting with matter and being degraded to optical photons. This suggests that the mass of the ejecta is small, and/or the radioactive material has been mixed throughout the ejecta. The peculiar "type IIb" SN 1993J, which faded at a similar rate of 0.02 mag per day (R94), is thought to have had an envelope mass of only $1.6 - 4.6 M_\odot$ (see Table 4 of Wheeler & Filippenko 1995).

Another clue to the mass of the ejecta in SN 1994I is the width of the peak of the light curve. As Figure 14 shows, the peak of its light curve is substantially narrower than those of two other SNe with relatively low-mass envelopes: SN 1993J (see above) and SN 1994D (which, as a type Ia, presumably had $M_{\rm ejecta} \leq 1.4 M_\odot$). Since the light curve at this time is driven by the diffusion of energy produced by the radioactive decay of ^{56}Ni to ^{56}Co, its width is dependent on the amount of material through which the energy must flow. A massive envelope increases the diffusion time and leads to a broad peak near maximum light. A skimpy envelope, on the other hand, allows photons to escape more quickly from the inner, ^{56}Ni-rich layers in which they are produced, yielding a narrow peak. Other factors can affect the light curve shape: if radioactive material is mixed into the outer layers in the explosion, its energy will escape more quickly from the envelope, producing a short-lived maximum.

6. Extinction

The color curves of SN 1994I suggest that the object was observed through significant amounts of interstellar material. We examine here the several methods which have been used to estimate the amount of extinction; impatient readers can skip directly to Table 8 for a summary.

Burstein & Heiles (1984) derive zero extinction along the line of sight to M51, based on the HI emission inside our own Milky Way Galaxy, implying that most of the material must be in M51. High-resolution observations of the Na I D absorption features by Ho & Filippenko (1995) confirm that most of the material lies in M51. They measure equivalent widths $W_\lambda(D1) = 1952 \pm 11$ mÅ and $W_\lambda(D2) = 2461 \pm 11$ mÅ by summing many components along the line of sight. If one were to apply the relationship derived in R94 relating the width of the sodium lines to color excess, one would calculate $E(B-V) = 0.92$ mag. However, since that relationship was extracted from observations of stars behind low-density regions in the Milky Way, it might not apply to high-density clouds in another galaxy; in addition, the widths of the saturated Na I lines in the spectrum of SN 1994I are three times larger than any used to derive the above formulae.

Ho & Filippenko, aware of these problems, fit the shape of each component in the Na I lines to calculate the sodium column density in each. They then convert to column density of neutral hydrogen, and use relationships between log $N(H)$ and color excess to derive $A_V = 3.1^{+3.1}_{-1.5}$ mag to SN 1994I. They point out several possible systematic errors in their analysis, and argue that this value is an overestimate; they prefer $1.0 \leq A_V \leq 2.0$ mag.

Baron *et al.* (1995) fit the observed spectra of SN 1994I at several epochs to models of an atmosphere of a C+O star. From the earliest spectra, they find $0.9 \leq A_V \leq 1.4$ mag, with values near the upper limit being favored at late times.

Iwamoto *et al.* (1994) compare the observed colors of SN 1994I to their own models, based on the explosion of a C+O star. They quote a value of $A_V = 1.4 \pm 0.25$ mag.

We will adopt a value of $A_V = 1.4 \pm 0.5$ mag for the remainder of this paper. Using the conversions from color excess to extinction listed in R94, this corresponds to $E(B-V) = 0.45 \pm 0.16$ mag. We list the extinction in each passband in Table 9. The large uncertainty in the extinction to this object will limit our ability to convert the apparent peak magnitudes to absolute ones, and to compare the intrinsic luminosity of SN 1994I to that of other supernovae.

7. Absolute magnitude

The distance to M51, surprisingly enough, has not been the subject of many inquiries. We were able to find only two distance determinations (other than those using the redshift and H_0) in the literature. Sandage & Tammann (1974b) used the sizes of the three largest H II regions in a set of Local Group galaxies to calibrate a relationship with some dependence on the type and luminosity class of the parent galaxy; they determined a distance modulus of $\mu = 29.9$ mag to M51. Georgiev *et al.* (1990) compared the distribution of apparent sizes and luminosities of young stellar associations in M33 and M51 to derive $\mu = 29.2$ mag. In addition, John Tonry (1995) kindly provided a preliminary distance to NGC 5195, the smaller galaxy interacting with M51, based on surface-brightness fluctuations (SBF). He finds a distance modulus of $\mu = 29.59 \pm 0.15$ to NGC 5195.

Since SN 1994I appeared, several authors have tried to use its properties to calculate the distance to its host galaxy. The results depend heavily on models of the explosion and their assumptions. Iwamoto *et al.* (1994) find that the observed light curve shapes best match theoretical ones when $\mu = 29.2 \pm 0.3$ mag and $A_V = 1.4 \pm 0.25$ mag. Baron *et al.* (1995) apply – with well-stated caveats – the Expanding Photosphere Method (Kirshner & Kwan 1974; Schmidt, Eastman, & Kirsher 1992) to the event and find $\mu = 29.6 + 5\log(t_r/9) \pm 0.5 \pm 0.7$ mag, where t_r is the rise time of the bolometric light curve, in days, and the quoted uncertainties are, first, those appropriate for formal fits of the data to their model, and, second, the external uncertainties in calibration and reddening; they assume $E(B-V) = 0.45$ mag. Looking at Tables 2 and 7, we see that our earliest detection of SN 1994I occurs 7.5 days before it peaks in the B-band. A slightly earlier observation places a strong upper limit on the SN's brightness 9.5 days before the B-band peak. We assume that the time of bolometric maximum occurs at the time of peak light in the

B-band (as R94 show is likely for the secondary peak of SN 1993J). Accepting their value of $t_r = 9$ days, we are left with $\mu = 29.6$.

It is clear that no measurement based on SN 1994I itself can be very precise, due to the large uncertainty in the reddening to the supernova. If similarly-large extinction were present in the stellar associations studied by Georgiev *et al.* (1990), and not taken into account, it would lead to an underestimation of the distance to M51 (implying $\mu > 29.2$ mag). The work by Sandage & Tammann (1974b) should be less affected by extinction, but their calibration of the sizes of H II regions may have systematic errors. Comparing their values (Sandage & Tammann 1974a) for the distances to some of their calibrating galaxies to more recent ones, we find evidence for overestimation of the distance scale (suggesting $\mu < 29.9$): they place M31 at $\mu = 24.84$ mag, whereas a recent review of a number of methods (de Vaucouleurs 1993) finds $\mu = 24.3$ mag, and their estimate of $\mu = 29.3$ mag for M101 is slightly higher than a value of $\mu = 29.1$ mag based on 4 Cepheids and 4 Miras (Alves & Cook 1995). We feel the SBF method is superior to the other methods considered here, in any case, and so give it the greatest weight in calculating a distance modulus to M51. We adopt $\mu = 29.6$, to which we will attach a very large uncertainty of 0.3 mag, in view of the preliminary nature of the SBF distance and the considerable difference between those produced by the other two methods.

Given this distance, the extinction adopted in the previous Section, and the apparent magnitudes at peak listed in Table 7, we can calculate the peak absolute magnitudes of SN 1994I, which we place in Table 10. Note that the uncertainties are dominated by the unknown extinction for all passbands except I. The range of likely values for the luminosity of this type Ic supernova is so large that detailed comparisons to other events seem pointless. We *can* say, at least, that SN 1994I appears to have been less luminous than a "normal" type Ia SN (R95 and references therein).

Using the machinery of R94[3], we can use this distance to convert the measured fluxes from SN 1994I into luminosity, creating a "quasi-bolometric" light curve (Figure 15). We corrected each magnitude for extinction, converted the magnitude into flux using the calibration of Bessell (1979), and summed all the fluxes (making a very minor correction for the area of overlap between the filters). Assuming a distance modulus of $\mu = 29.6$ mag to M51, we then translated the summed optical flux into a luminosity. Note that this "quasi-bolometric" luminosity does **not** include any contribution from the UV or IR, nor is it derived from any blackbody fit to the optical fluxes.

In our calculations, we use three values for the color excess to the SN: 0.30, 0.45, and 0.60 mag. The shape of the bolometric light curve at very early times depends significantly on the extinction. Note the difference in Figure 15 between the $UBVRI$ and $BVRI$ sums for the highest

---

[3]In the course of performing calculations for SN 1994I, we found an error in our routine that corrects for extinction. This error affected the analysis of SN 1993J in R94 in the following manner: in Tables 14 and 15, and in Figure 11, one should replace the label "$E(B-V) = 0.32$" with "$E(B-V) = 0.40$." The results for $E(B-V) = 0.08$ are correct as printed in R94. We thank Brian Schmidt for his attention to detail, which led to the discovery of this error.

value of color excess. Even after maximum brightness, on April 19, 1994 UT, the U-band still contributes about 10% of the summed optical flux. Tables 11 and 12 contain the quasi-bolometric luminosity of SN 1994I for each night in which we measured at least B, V, R, and I-band magnitudes.

8. Comparison to the type Ic SN 1987M

The only other type Ic SN for which we can find more than a handful of photometric data in the literature is SN 1987M. Filippenko, Porter, & Sargent (1990) published a set of light curves together with their detailed analysis of this object's spectra. Most of their photometry is constructed by applying a synthetic passband to flux calibrated spectra, and those points measured directly from images are in the Gunn-Thuan g and r passbands; it is therefore difficult to make a detailed comparison with our Johnson-Cousins $UBVRI$ data.

The light curve of SN 1987M is so sparse that one cannot confidently assign a date for maximum light; there is no indication that any measurement was made before the peak. Filippenko *et al.* suggest that the light curves are consistent with maximum brightness occurring at the time of discovery, September 21, 1987. When shifting the points for SN 1987M to find the best match to the light curves for SN 1994I, we found a fair match when we pushed the date of SN 1987M's maximum forward about 5 days, to September 26, 1987.

We compare the shapes of the matched light curves in Figures 16 and 17. Note that the Thuan-Gunn g filter has an effective wavelength of about 4930 Å, quite a bit longer than the Johnson B filter's 4400 Å. We might therefore expect the g curve of SN 1987M to fall more slowly than its B light curve, but Figure 16 shows that the difference is small. Both appear similar to the B-band light curve of SN 1994I, although the last datum for SN 1987M, about 95 days after maximum light, is about 0.5 mag fainter. The Cousins R and Thuan-Gunn r have nearly identical effective wavelengths, so SN 1987M's decidedly slower decline from peak light, seen in Figure 17, may represent a real difference in its physical properties. There is, however, no indication that either type Ic SN displayed a "shoulder" in the R-band, distinguishing both from "normal" type Ia SNe, but not from subluminous events such as SNe 1991bg (Filippenko *et al.* 1992; Leibundgut *et al.* 1993) and 1992K (Hamuy *et al.* 1994).

In Figure 11, we compare the $(B-V)$ colors of the two supernovae, again shifting the data for SN 1987M forwards by five days. We warn the reader that we have made many approximations to present this comparison, which must be qualitative, at best. If the intrinsic color of SN 1987M was similar to that of SN 1994I, then it must have suffered a greater amount of extinction than SN 1994I. On the other hand, Filippenko *et al.* measured the (unresolved) absorption lines of Na I D to have equivalent width of ~ 2.1 Å, while the two Na I D lines in the spectrum of SN 1994I had a summed equivalent width of ~ 4.4 Å (see Section 6), much larger than that of SN 1987M. This puzzle seems to imply that that either SN 1987M was intrinsically redder than SN 1994I, or that the gas-to-dust ratio and/or the properties of interstellar dust in NGC 5194 do not match those in NGC 2715.

9. Conclusions

We have collected a large set of observations of the type Ic SN 1994I in M51, including the earliest known detections and earlier upper limits, and reduced them to a common system. In order to minimize the contamination from the bulge of M51, we scaled and subtracted images of the galaxy alone from those containing the supernova. Our light curves document the behavior of SN 1994I in the optical from 9 days before maximum light to 120 days later.

We contribute two pieces of evidence that support the hypothesis that the mass of ejecta in SN 1994I was very small. First, the light curves have peaks much less broad than those of other SNe, even type Ia. Second, light in the VRI passbands faded at a rate about twice as fast as the decay rate of ^{56}Co. Theoretical models of an exploding C+O star (Iwamoto *et al.* 1994; Nomoto, Iwamoto, & Suzuki 1995) favor ejecta masses of only $0.5 - 0.9 M_{\odot}$.

Our best estimate for the reddening to the supernova, $E(B-V) = 0.45 \pm 0.16$, cannot be made very precise. The large and uncertain extinction due to material in its host galaxy renders the colors and absolute magnitudes of SN 1994I unreliable. It is probable that SN 1994I was redder and fainter at peak light than "typical" type Ia SNe, but one can say little more with confidence. Although the shapes of the light curves of SN 1994I are reasonably close to those of its fellow type Ic SN 1987M, there is evidence that the intrinsic colors of these two SNe may have been quite different.

Many people helped to spread the news of SN 1994I and kept us all informed. We especially thank Brian Skiff, Alejandro Clocchiatti, Taichi Kato and Bjorn Granslo. David Schlegel acquired a late-time image at Lick for us. Harold Corwin and Gerard de Vaucouleurs provided very useful background information. Jost Jahn and Tim Spuck provided vital communications and good advice to the authors. The Hands-On Universe project gave HT and MS access to the Leuschner Observatory facilities. We thank the referee, Brian Schmidt, for providing many suggestions which have improved this paper, even though he made us do a lot of extra work. MWR thanks the Department of Astrophysical Sciences at Princeton University. We are grateful to Sun Microsystems, Inc. (Academic Equipment Grant Program) and to Photometrics, Ltd. for equipment donations that were vital to the acquisition and reduction of data at Leuschner Observatory. Financial support for this research was provided to AVF and his group at UC Berkeley through NSF Grant Nos. AST-8957063, AST-9115174, and AST-9417213.

A. Photometric solutions for Leuschner and Lick

On 1995 April 24 UT, we used the 1-m Nickel telescope at Lick Observatory to observe the field of SN 1994I and five multi-star fields from the list of Landolt (1992) in $BVRI$. Using the `photcal` task in IRAF, we calculated a photometric solution for each passband of the form

$$V = v + v1 + v2 * X + v3 * (b - v) + v4 * X * (b - v)$$

where V denotes a standard magnitude, b and v instrumental values, and X the airmass. We list the solutions and their formal uncertainties below:

$$\begin{aligned}
B &= v \; +(b-v) && + 5.23 + 0.31X - 0.06(b-v) - 0.008X(b-v) \\
V &= v && +4.92 + 0.20X + 0.04(b-v) - 0.005X(b-v) \\
R &= v \; -(v-r) && + 4.86 + 0.13X + 0.04(v-r) + 0.0008X(v-r) \\
I &= v \; -(v-r) - (r-i) && + 4.91 + 0.11X + 0.07(r-i) - 0.05X(r-i).
\end{aligned}$$

For the Leuschner 50-cm telescope, we observed the M67 "dipper" asterism on April 1 and April 6, 1993, and on January 7, October 8 and October 29, 1994, to determine the first-order color terms which transform instrumental magnitudes to the standard Johnson-Cousins system. The terms C_V, C_{BV}, etc., are the differences between the zero-points of the instrumental and standard magnitudes, which vary from night to night. Since we always measured the brightness of SN 1994D relative to that of star A, these terms were not involved in the photometric solutions. We include second-order color-dependent extinction corrections *only* for instrumental B-band measurements, as described in the Appendix to R94; we denote the extinction-corrected B-band instrumental values by b^0 in the equations below. For the Leuschner 50-cm telescope, we find

$$\begin{aligned}
V &= v + && 0.02(v-i) + C_V \\
(B-V) &= && 1.15(b^0 - v) + C_{BV} \\
(U-B) &= && 1.20(u - b^0) + C_{UB} \\
(V-R) &= && 0.87(v-r) + C_{VR} \\
I &= i + && 0.05(v-i) + C_I.
\end{aligned}$$

We used images of M67 taken on October 31, November 8, November 11, and November 13, 1994, to calculate the color terms for the Leuschner 76-cm telescope, finding

$$\begin{aligned}
V &= v + && 0.01(v-i) + C_V \\
(B-V) &= && 1.16(b^0 - v) + C_{BV} \\
(V-R) &= && 0.88(v-r) + C_{VR} \\
I &= i + && 0.02(v-i) + C_I.
\end{aligned}$$

REFERENCES

Alves, D. R., & Cook, K. H. 1995, AJ, 110, 192

Baron, E., Hauschildt, P. H., Branch, D., Kirshner, R. P., & Filippenko, A. V. 1995 MNRAS, submitted

Bessell, M. S. 1979, PASP, 91, 589

Burstein, D., & Heiles, C. 1984, ApJS, 54, 33

Clocchiatti, A., Brotherton, M., Harkness, R. P., & Wheeler, J. C. 1994, IAU Circ. No. 5972

Corwin, H. 1994, private communication

de Vaucouleurs, G. 1993, ApJ, 415, 10

Filippenko, A. V., Porter, A. C., & Sargent, W. L. W., 1990, AJ, 100, 1575

Filippenko, A. V. *et al.* 1992, AJ, 104, 1543

Filippenko, A. V., Matheson, T., & Barth, A. J. 1994, IAU Circ. No. 5964

Filippenko, A. V. *et al.* 1995, ApJ, 450, L11

Georgiev, Ts. B., Getov, R. G., Zamanova, V. I., & Ivanov, G. R. 1990, Pis. Astr. Zh., 16, 979

Hamuy, M. et al. 1991, AJ, 102, 208

Hamuy, M. et al. 1994, AJ, 108, 2226

Ho, L. C., & Filippenko, A. V. 1995, ApJ, 444, 165

Iwamoto, K., Nomoto, K., Höflich, P., Yamaoka, H., Kumagai, S., & Shigeyama, T. 1994, ApJ, 437, L115

Kirshner, R. P., & Kwan, J. 1974, ApJ, 193, 27

Kirshner, R., & SINS team 1994, IAU Circ. No. 5981

Landolt, A. U. 1992, AJ, 104, 340

Leibundgut, B., *et al.* 1993, AJ, 105, 301

Lee, M. G., Kim, E., Kim, S. C., Kim, S.-L., Park, W.-K., & Pyo, T. S. 1995, Jour. Kor. Astr. Soc., in press

Morrison, L. V., & Argyle, R. W. 1994, IAU Circ. No. 5989

Nomoto, K., Iwamoto, K, & Suzuki, T. 1995, Physics Reports 256, 173

Phillips, M. M. 1993, ApJ, 413, L105

Puckett, T., Armstrong, J., Johnson, W., Millar, D., Berry, R., & Kushida, R. 1994, IAU Circ. No. 5961

Richmond, M. W., Treffers, R. R., & Filippenko, A. V. 1993, PASP, 105, 1164

Richmond, M. W., Treffers, R. R., Filippenko, A. V., Paik, Y., Leibundgut, B., Schulman, E., & Cox, C. V. 1994, AJ, 107, 1022 (R94)

Richmond, M. W. *et al.* 1995, AJ 109, 2121 (R95)

Rupen, M. P., Sramek, R. A., Van Dyk, S. D., Weiler, K. W., & Panagia, N. 1994, IAU Circ. No. 5963

Sandage, A., & Tammann, G. A., 1974a, ApJ, 190, 525

Sandage, A., & Tammann, G. A., 1974b, ApJ, 194, 559

Schmidt, B., Challis, P., & Kirshner, R. 1994, IAU Circ. No. 5966

Schmidt, B. & Kirshner, R. 1994a, IAU Circ. No. 5962

Schmidt, B. & Kirshner, R. 1994b, private communication

Thompson, G. D., & Bryan, J. T. Jr. 1989, Supernova Search Charts and Handbook (Cambridge: Cambridge University Press)

Tonry, J. 1995, private communication

Turatto, M. & Zanin, C. 1994, IAU Circ. No. 5971

Wheeler, J. C., Harkness, R. P., Clocchiatti, A., Benetti, S., Brotherton, M. S., Depoy, D. L., & Elias, J. 1994, ApJ, 436, L135

Wheeler, J. C., & Filippenko, A. V. 1995, in Supernovae and Supernova Remnants, ed. R. M. McCray and Z. W. Li (Cambridge: Cambridge Univ. Press)

Yokoo, T., Arimoto, J., Matsumoto, K., Takahashi, A., & Sadakane, K. 1994, PASJ, 46, L191

This preprint was prepared with the AAS LaTeX macros v3.0.

Table 1. Johnson-Cousins magnitudes of comparison stars

star	U	B	V	R	I	source
A	14.14*	14.05	13.44	13.08	12.81	Corwin 1994
A	$\cdots$	$14.005^* \pm 0.004$	$13.420^* \pm 0.002$	$13.067^* \pm 0.003$	$12.730^* \pm 0.004$	Lick
B	$\cdots$	16.57:	15.09:	14.39:	13.65:	Corwin 1994
B	$\cdots$	16.339 ± 0.017	15.096 ± 0.007	14.331 ± 0.009	13.680 ± 0.005	Lick
C	$\cdots$	15.751 ± 0.017	15.212 ± 0.010	14.857 ± 0.013	14.497 ± 0.010	Lick
D	$\cdots$	16.168 ± 0.016	15.266 ± 0.007	14.746 ± 0.009	14.200 ± 0.005	Lick

*Adopted as primary comparison star values.

Table 2. Early observations of SN 1994I

UT Date	JD[a]	V	R	source
Mar 28.44	9439.94		≥ 18.2	Leuschner 76-cm
Mar 29.39	9440.89	≥ 18.82		Leuschner 76-cm
Mar 31.43	9442.93	16.41 ± 0.25		Leuschner 76-cm
Mar 31.96	9443.46	15.46 ± 0.47		Luebeck 49-cm unfiltered
Apr 02.02	9444.52		13.97 ± 0.25	Bustamante 20-cm unfiltered

[a]Julian Date − 2,440,000.

Table 3. Internal accuracy of differential magnitudes

difference	B	V	R	I	telescope
A-B	0.11	0.04	0.02	0.01	Leuschner 50-cm
A-B	···	0.10	0.08	0.03	Leuschner 76-cm
A-C	0.05	0.03	0.02	0.02	Leuschner 50-cm
A-C	···	0.13	0.07	0.06	Leuschner 76-cm
A-D	0.13	0.05	0.04	0.05	Leuschner 50-cm
A-D	···	0.10	0.05	0.04	Leuschner 76-cm

Table 4. Leuschner 50-cm data[a] on SN 1994I

UT Date	JD[b]	U[c]	B	V	R	I	conditions
Apr 02.45	9444.95	···	14.41 (03)	14.03 (01)	13.87 (02)	13.78 (01)	clouds
Apr 05.39	9447.89	13.88 (06)	13.95 (02)	13.21 (01)	13.06 (02)	12.90 (01)	
Apr 11.44	9453.94	···	14.06 (03)	13.03 (01)	12.76 (02)	12.52 (01)	
Apr 12.32	9454.82	14.59 (09)	14.18 (03)	13.10 (01)	12.78[d](01)	12.54 (01)	
Apr 13.38	9455.88	14.91 (15)	14.56 (02)	13.30 (01)	12.95 (02)	12.65 (01)	
Apr 14.34	9456.84	···	14.56 (02)	13.30 (01)	12.95 (02)	12.65 (01)	poor seeing
Apr 18.35	9460.85	···	15.28 (03)	13.93 (01)	13.41 (02)	13.00 (01)	
Apr 19.32	9461.82	15.97 (21)	15.40 (04)	14.08 (02)	13.53 (03)	13.10 (01)	
Apr 27.31	9469.81	···	···	14.95 (04)	14.39 (05)	13.81 (02)	slight trails
May 03.31	9475.81	···	16.28 (10)	15.45 (06)	14.80 (08)	14.13 (02)	clouds, V trailed
May 06.30	9478.80	···	···	15.43 (02)	14.90 (03)	14.27 (01)	
May 08.33	9480.83	···	···	15.71 (16)	15.04 (21)	14.32 (01)	V double exp.
May 09.31	9481.81	···	16.61 (08)	15.56 (02)	15.03 (03)	14.37 (02)	
May 13.27	9485.77	···	16.56 (11)	15.71 (04)	15.18 (05)	14.51 (01)	
May 14.25	9486.75	···	16.76 (08)	15.70 (04)	15.21 (05)	···	poor seeing
May 18.20	9490.70	···	16.58 (16)	15.90 (03)	15.41 (07)	14.62 (01)	clouds
May 21.32	9493.82	···	16.88 (07)	15.94 (02)	15.45 (03)	14.74 (02)	
May 22.37	9494.87	···	16.86 (09)	15.89 (01)	15.49 (02)	14.74 (06)	
May 29.36	9501.86	···	17.21 (14)	16.18 (07)	15.73 (09)	15.00 (03)	
May 30.29	9502.79	···	17.06 (06)	16.24 (02)	15.75 (04)	15.04 (02)	
Jun 01.31	9504.71	···	16.93 (17)	16.21 (04)	15.74 (06)	15.08 (02)	poor seeing
Jun 02.44	9505.94	···	···	16.26 (07)	15.78 (12)	15.05 (04)	poor seeing
Jun 08.21	9511.71	···	17.21 (18)	16.48 (04)	15.99 (06)	15.30 (02)	
Jun 11.21	9514.71	···	···	16.58 (04)	16.04 (06)	15.37 (05)	

[a]Parantheses enclose uncertainty, in hundredths of a magnitude.

[b]Julian Date − 2,440,000, at midpoint of sequence of images.

[c]Extracted via pure aperture photometry.

[d]Star C used as comparison, A not in frame.

Table 5. Leuschner 76-cm data[a] on SN 1994I

UT Date	JD[b]	B	V	R	I	conditions
Apr 02.52	9445.02	···	14.13 (05)	13.77 (11)	13.75 (01)	clouds
Apr 03.37	9445.87	···	13.78 (04)	13.50 (10)	13.43 (02)	clouds
Apr 04.42	9446.92	13.97 (08)	13.39 (01)	13.21 (02)	13.09 (01)	
Apr 05.47	9447.97	···	13.20 (00)	12.98 (00)	12.86 (01)	
Apr 07.36	9449.86	13.68 (21)	12.99 (01)	12.72 (02)	12.60 (01)	
Apr 10.45	9452.95	13.81 (07)	12.91 (01)	12.62 (02)	12.49 (01)	
Apr 11.45	9453.95	14.02 (04)	13.01 (01)	12.70 (02)	12.52 (01)	
Apr 12.35	9454.85	14.23 (04)	13.13 (02)	12.74 (03)	12.56 (00)	
Apr 13.38	9455.88	14.35 (03)	13.14 (01)	12.77 (02)	12.59 (01)	
Apr 14.33	9456.83	···	13.37 (02)	12.92 (03)	12.62 (01)	poor seeing
Apr 15.32	9457.82	14.75 (02)	13.46 (01)	13.04 (02)	12.72 (01)	
Apr 21.35	9463.85	···	14.29 (02)	13.69 (03)	13.23 (01)	faint "bands"[c]
Apr 27.32	9469.82	16.00 (32)	14.90 (03)	14.36 (04)	13.76 (01)	bands
Apr 28.30	9470.80	15.97 (30)	15.11 (01)	14.50 (01)	13.96 (02)	bands, clouds
Apr 29.29	9471.79	···	15.12 (04)	14.58 (06)	13.96 (02)	bands, poor seeing
May 02.29	9474.79	···	15.27 (03)	14.69 (05)	14.09 (02)	
May 03.29	9475.79	···	15.26 (12)	14.81 (19)	14.10 (02)	clouds
May 04.28	9476.78	···	15.26 (11)	14.86 (15)	14.16 (03)	clouds
May 06.31	9478.81	···	15.46 (03)	14.99 (04)	14.30 (04)	
May 08.38	9480.78	···	15.55 (04)	15.03 (06)	14.33 (02)	
May 13.26	9485.76	···	15.69 (07)	15.27 (10)	14.55 (01)	
May 21.25	9493.75	···	16.05 (11)	15.46 (16)	14.80 (04)	
May 22.27	9494.77	···	16.00 (10)	15.48 (16)	14.81 (03)	
May 23.28	9495.78	···	16.03 (21)	15.50 (29)	14.91 (02)	clouds

[a]Parantheses enclose uncertainty, in hundredths of a magnitude.

[b]Julian Date − 2,440,000, at midpoint of sequence of images.

[c]Faint curved bands visible on image, probably flatfielding problems.

Table 6. Lick data[a] on SN 1994I

UT Date	JD[b]	B	V	R	I
Apr 11.47	9453.97	···	···	12.71 (01)	···
Apr 12.37	9454.87	14.11 (01)	13.10 (00)	12.75 (00)	12.50 (01)
Apr 13.50	9456.00	14.37 (01)	13.26 (00)	12.85 (01)	12.58 (00)
May 14.46	9486.96	16.78 (04)	15.77 (02)	15.25 (03)	14.54 (00)
Jun 11.38	9514.88	17.48 (08)	···	15.94 (04)	···
Jul 13.32	9546.82	17.95 (26)	···	···	···
Jul 14.30	9547.80	18.05 (13)	17.23 (08)	16.46 (08)	15.95 (05)
Aug 07.21	9571.71	18.10 (18)	17.60 (06)	16.93 (09)	16.34 (05)

[a]Parantheses enclose uncertainty, in hundredths of a magnitude.

[b]Julian Date – 2,440,000, at midpoint of sequence of images.

Table 7. Peak apparent magnitudes of SN 1994I

	U[a]	B	V	R	I
JD[b]	9449.5 ± 0.1	9450.56 ± 0.04	9451.44 ± 0.03	9451.92 ± 0.04	9452.44 ± 0.08
UT	Apr 07.0	Apr 08.06	Apr 08.94	Apr 09.42	Apr 09.94
Mag[c]	13.82 ± 0.04	13.77 ± 0.02	12.91 ± 0.02	12.65 ± 0.02	12.50 ± 0.02
Δm_{15}[d]	···	2.07 ± 0.03	1.74 ± 0.02	1.46 ± 0.02	1.08 ± 0.02

[a]Time and value of peak based on fit to 50-cm and CfA data.

[b]Julian Day $-2,440,000$, measured at peak of polynomial fit.

[c]Based on polynomial fit to points within JD 9444-9458.

[d]Decline from peak to value 15 days later.

Table 8. Estimates of color excess (mag) to SN 1994I

method	E(B-V)	calibration	source
W_λ (Na D) to E(B-V)	0.92	Sembach et al. 1993	Richmond et al. 1994
log N(Na I) to log N(H) to E(B-V)	$1.0^{+1.0}_{-0.5}$	Ferlet et al. 1985 Spitzer 1978	Ho & Filippenko 1995
fits to model SN spectra	$0.29 - 0.45$		Baron et al. 1995
fits to model SN light curves	0.45 ± 0.16		Iwamoto et al. 1994

Table 9. Adopted extinction (mag) to SN 1994I

E(B-V)	A_U	A_B	A_V	A_R	A_I
0.45	2.21	1.85	1.40	1.04	0.68

Table 10. Absolute[a] peak magnitudes for SN 1994I

U	B	V	R	I
-17.99 ± 0.84	-17.68 ± 0.73	-18.09 ± 0.58	-17.99 ± 0.48	-17.78 ± 0.38

[a]Assuming $\mu = 29.6 \pm 0.3$ mag and $E(B-V) = 0.45$ mag.

Table 11. UBVRI quasi-bolometric luminosity[a] of SN 1994I (erg/s)

JD[b]	E(B-V)=0.30	E(B-V)=0.45[c]	E(B-V)=0.60
9447.89	1.465e+42	2.373e+42	3.917e+42
9454.82	1.455e+42	2.260e+42	3.571e+42
9455.88	1.182e+42	1.815e+42	2.839e+42
9461.82	6.285e+41	9.468e+41	1.450e+42

[a]Assuming distance to M51 is 8.32 Mpc ($\mu = 29.6$ mag).

[b]Julian Date − 2,440,000, at midpoint of sequence of images.

[c]Preferred value.

Table 12. BVRI quasi-bolometric luminosity[a] of SN 1994I (erg/s)

JD[b]	E(B-V)=0.30	E(B-V)=0.45[c]	E(B-V)=0.60
9444.95	6.450e+41	1.015e+42	1.619e+42
9446.92	1.091e+42	1.700e+42	2.682e+42
9447.89	1.214e+42	1.879e+42	2.944e+42
9449.86	1.571e+42	2.427e+42	3.795e+42
9452.95	1.605e+42	2.453e+42	3.798e+42
9453.94	1.399e+42	2.124e+42	3.265e+42
9453.95	1.444e+42	2.194e+42	3.374e+42
9454.82	1.324e+42	2.003e+42	3.065e+42
9454.85	1.311e+42	1.978e+42	3.020e+42
9454.87	1.367e+42	2.069e+42	3.172e+42
9455.88	1.084e+42	1.624e+42	2.462e+42
9455.88	1.256e+42	1.889e+42	2.874e+42
9456.84	1.084e+42	1.624e+42	2.462e+42
9457.82	9.650e+41	1.440e+42	2.172e+42
9456.00	1.188e+42	1.786e+42	2.719e+42
9460.85	6.628e+41	9.799e+41	1.466e+42
9461.82	5.918e+41	8.749e+41	1.307e+42
9469.82	2.988e+41	4.429e+41	6.650e+41
9470.80	2.649e+41	3.959e+41	5.996e+41
9475.81	2.048e+41	3.046e+41	4.594e+41
9481.81	1.657e+41	2.457e+41	3.692e+41
9485.77	1.510e+41	2.257e+41	3.419e+41
9486.96	1.385e+41	2.056e+41	3.091e+41
9490.70	1.331e+41	1.999e+41	3.048e+41
9493.82	1.184e+41	1.764e+41	2.664e+41
9494.87	1.189e+41	1.774e+41	2.683e+41
9501.86	9.170e+40	1.363e+41	2.052e+41
9502.79	9.236e+40	1.383e+41	2.099e+41
9504.71	9.534e+40	1.437e+41	2.197e+41
9511.71	7.534e+40	1.133e+41	1.728e+41
9547.80	4.094e+40	6.088e+40	9.179e+40
9571.71	3.046e+40	4.603e+40	7.057e+40

[a]Assuming distance to M51 is 8.32 Mpc ($\mu = 29.6$ mag).

[b]Julian Date − 2,440,000, at midpoint of sequence of images.

[c]Preferred value.

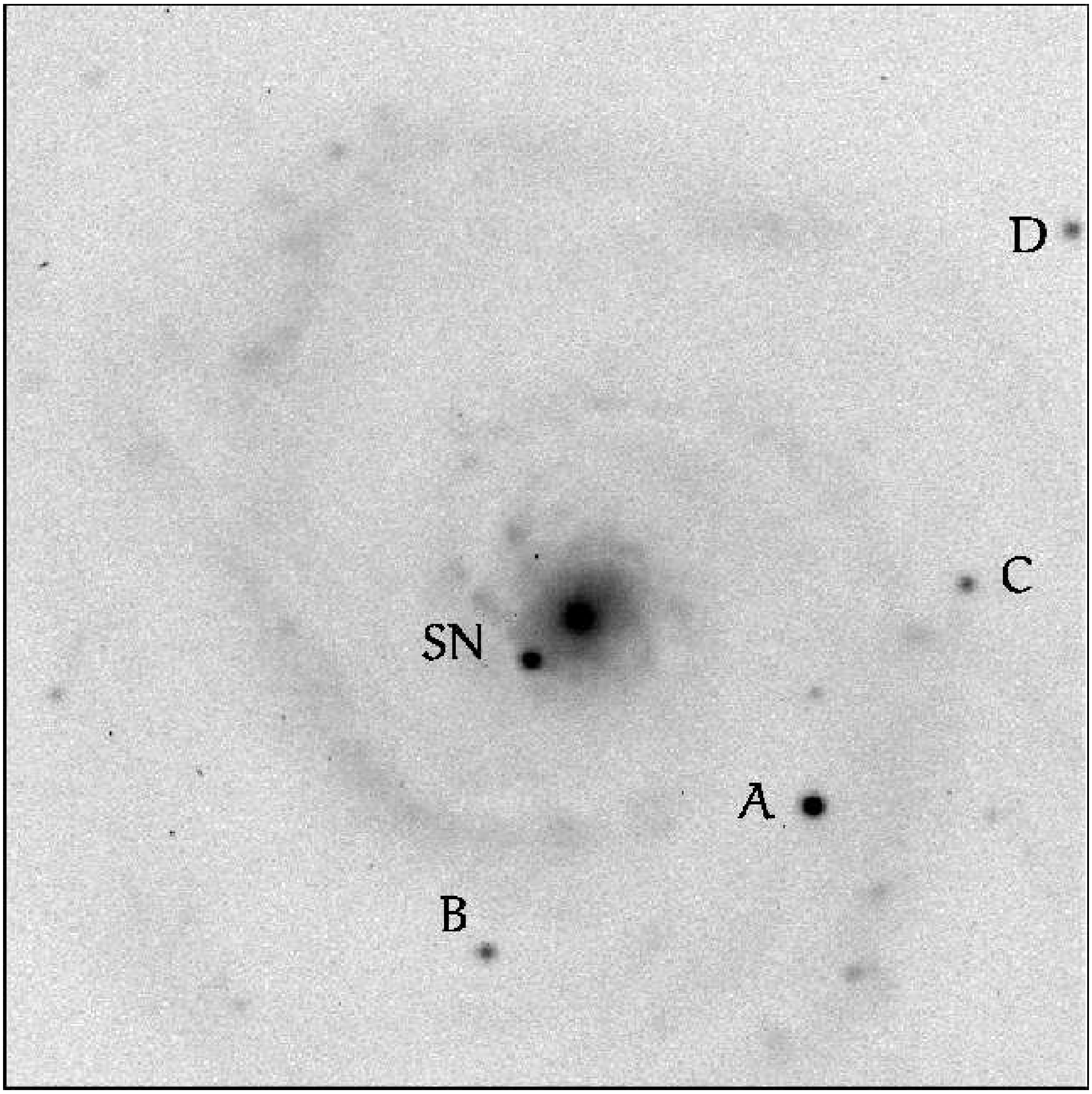

Fig. 1.— V-band image of M51 (= NGC 5194) and SN 1994I taken Apr 2, 1994, with comparison stars marked. North is up and East to the left. The field of view is about $5\farcm3 \times 5\farcm3$. SN 1994I is about $19''$ from the nucleus of M51.

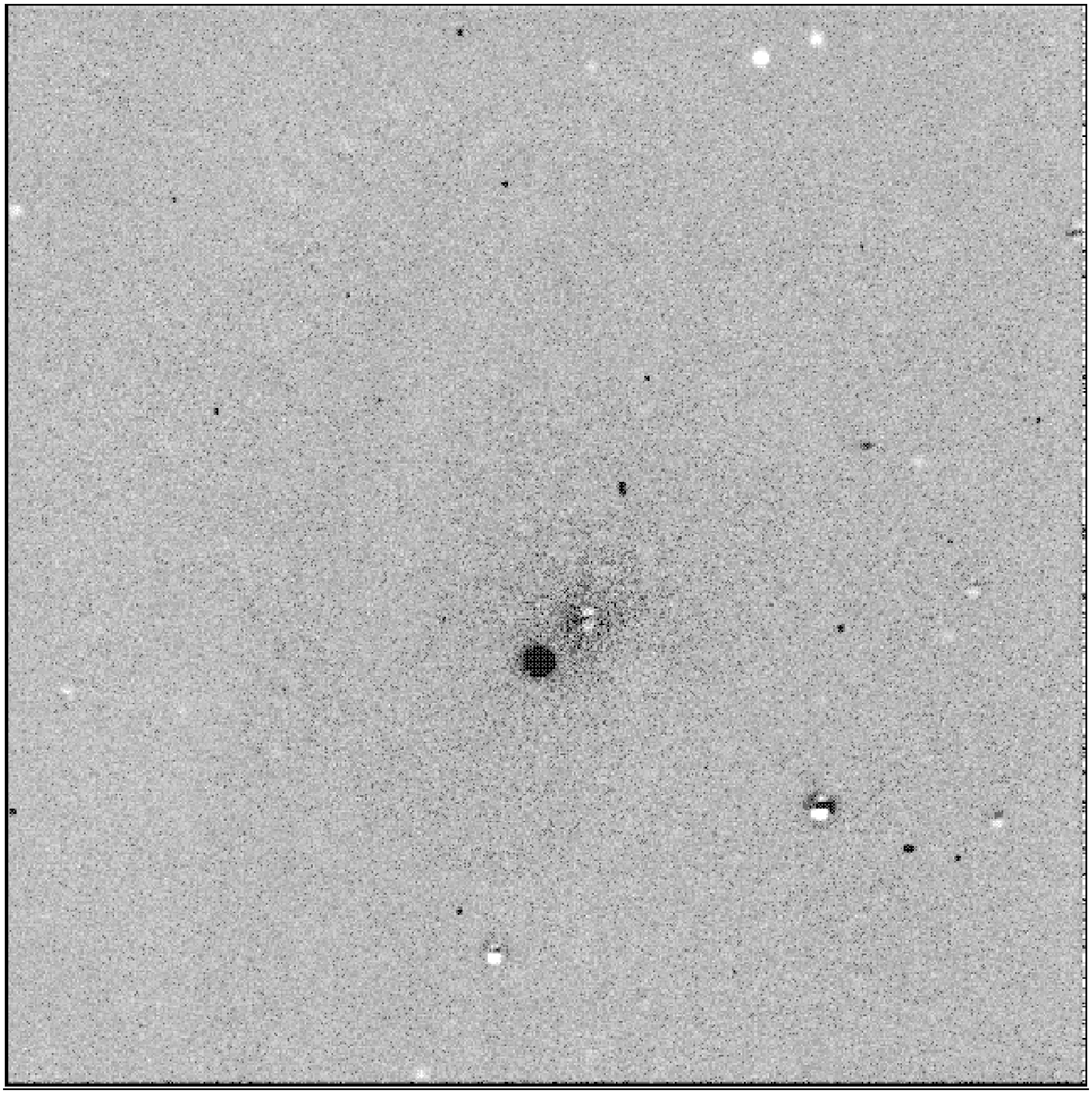

Fig. 2.— I-band image of M51 and SN 1994I taken Apr 5, 1994, after application of the "tempsub" technique. Postive features are dark and negative ones white. North is up and East to the left.

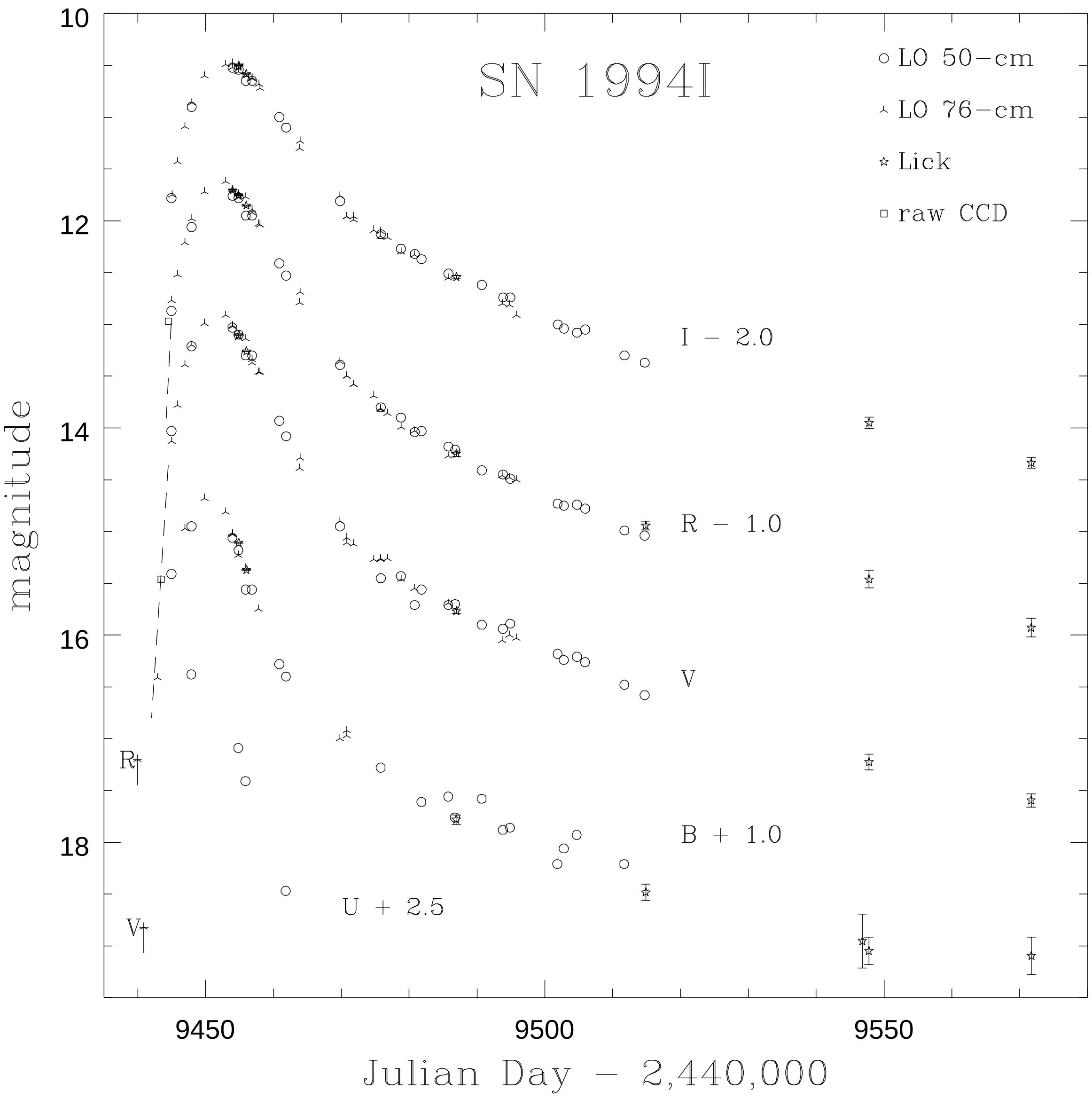

Fig. 3.— *UBVRI* light curves of SN 1994I.

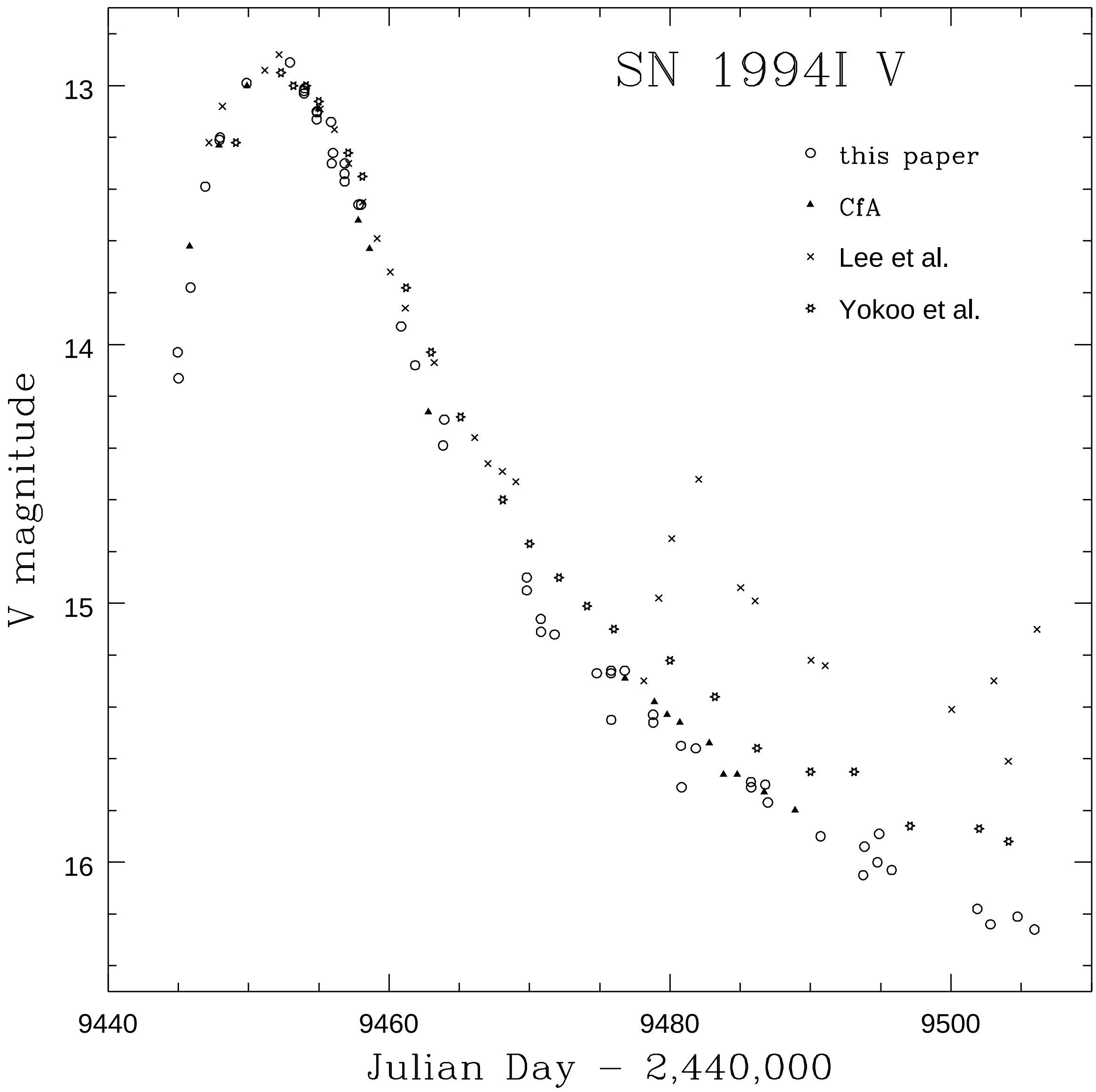

Fig. 4.— Comparison of the V light curves of SN 1994I obtained by this paper, Schmidt & Kirshner "CfA" (1994b), Yokoo *et al.* (1994) and Lee *et al.* (1995).

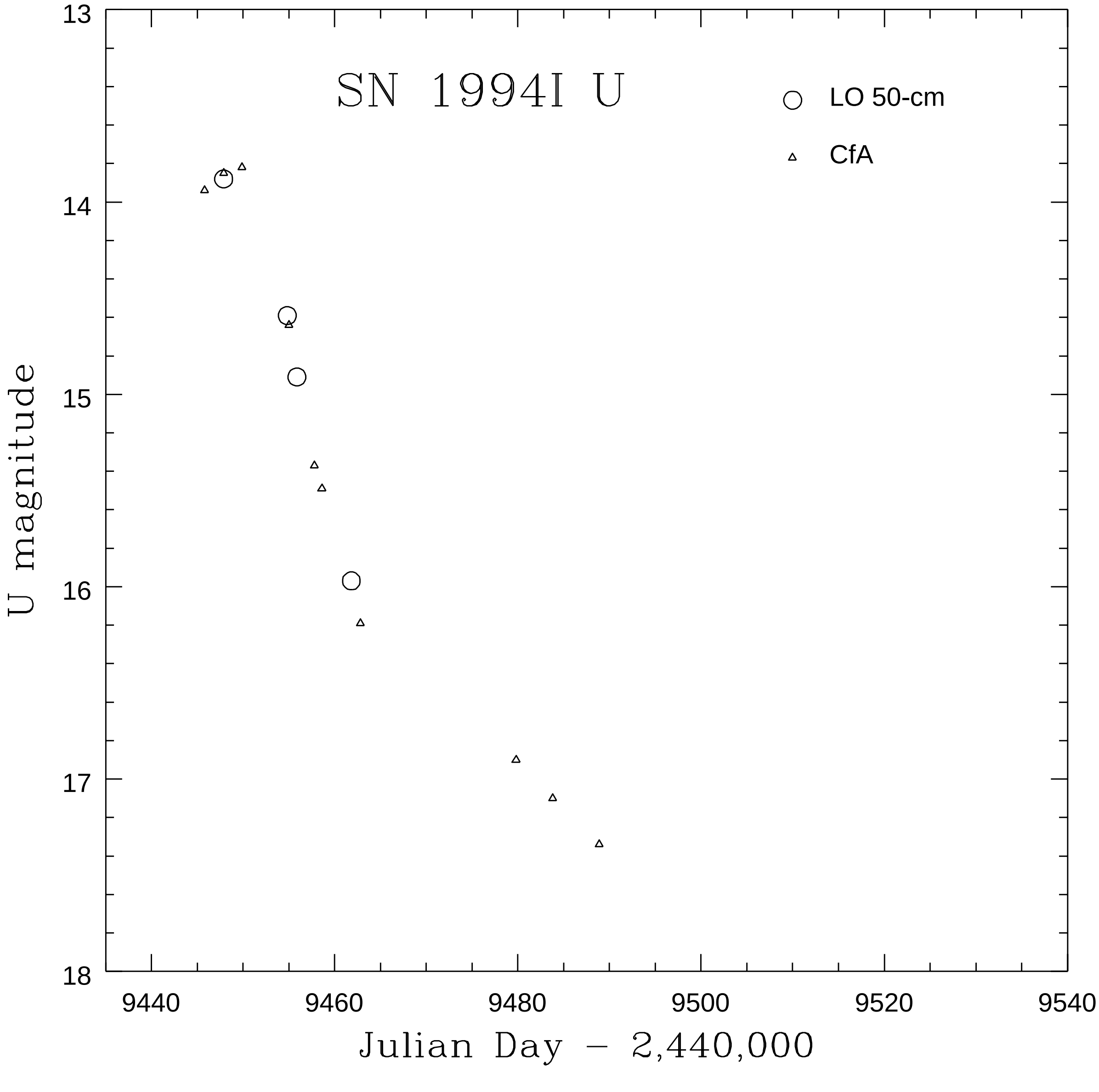

Fig. 5.— U light curve of SN 1994I. The data labelled "CfA" were provided by Schmidt & Kirshner (1994b).

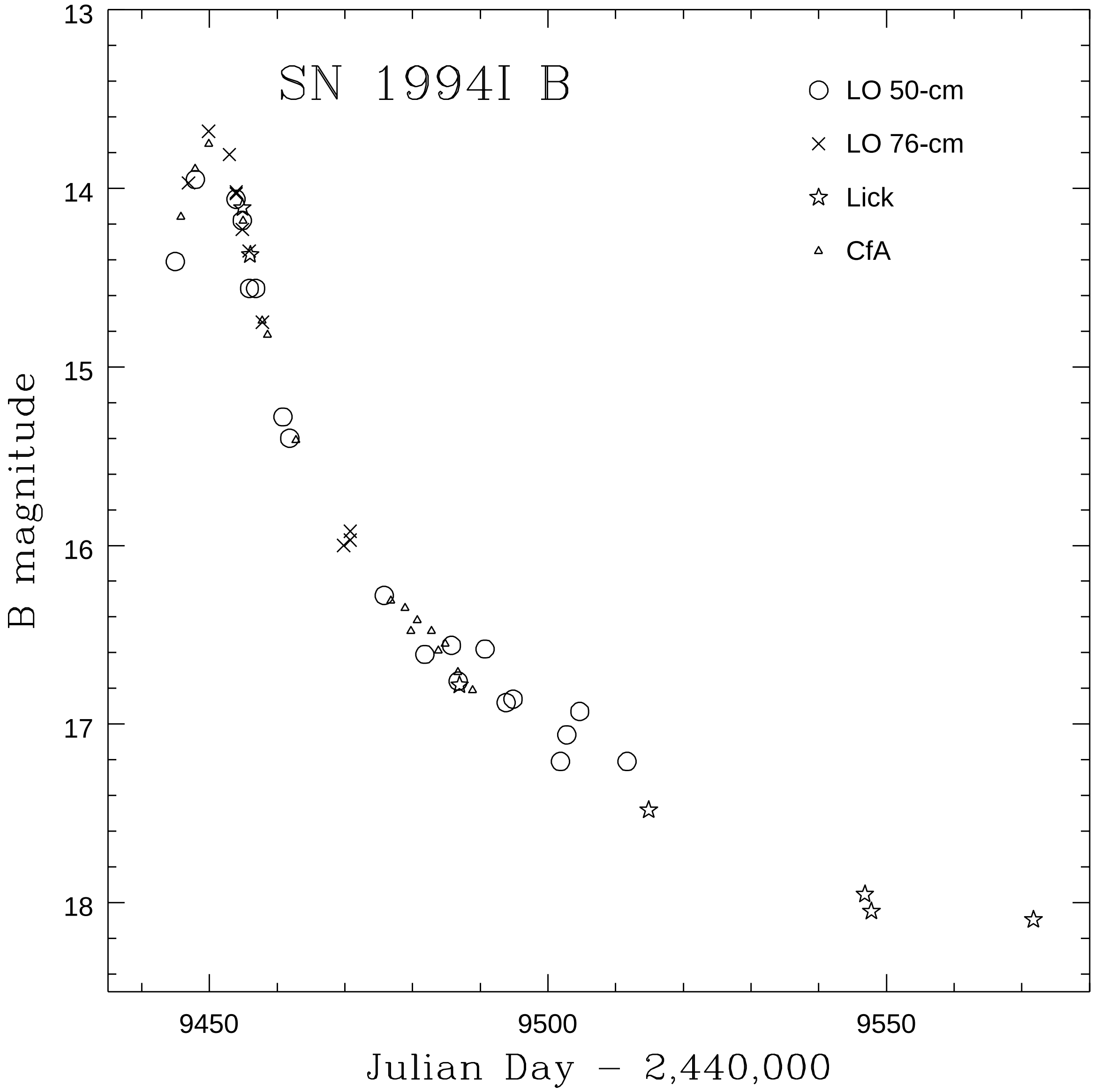

Fig. 6.— *B* light curve of SN 1994I. The data labelled "CfA" were provided by Schmidt & Kirshner (1994b).

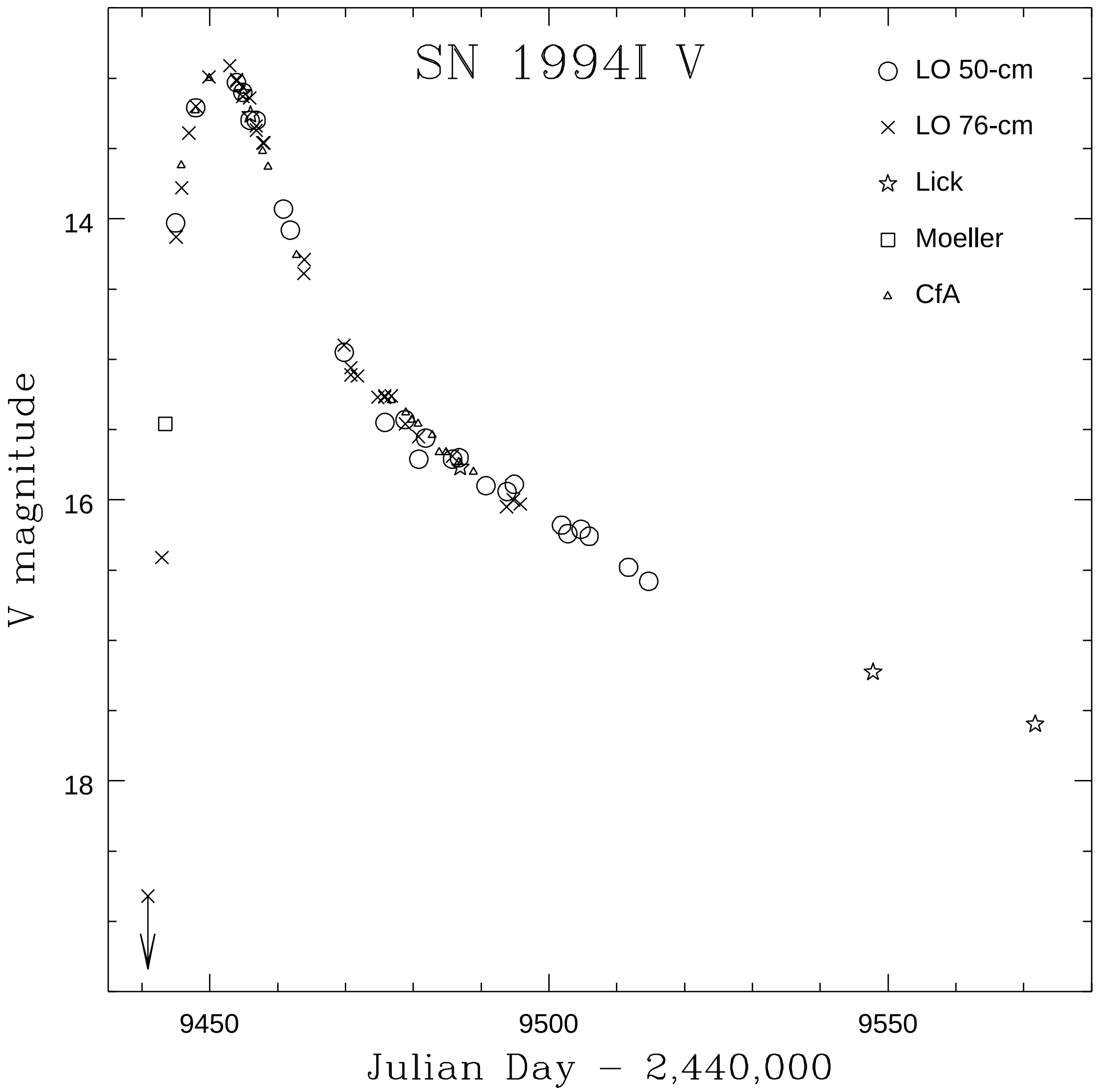

Fig. 7.— *V* light curve of SN 1994I. The data labelled "CfA" were provided by Schmidt & Kirshner (1994b).

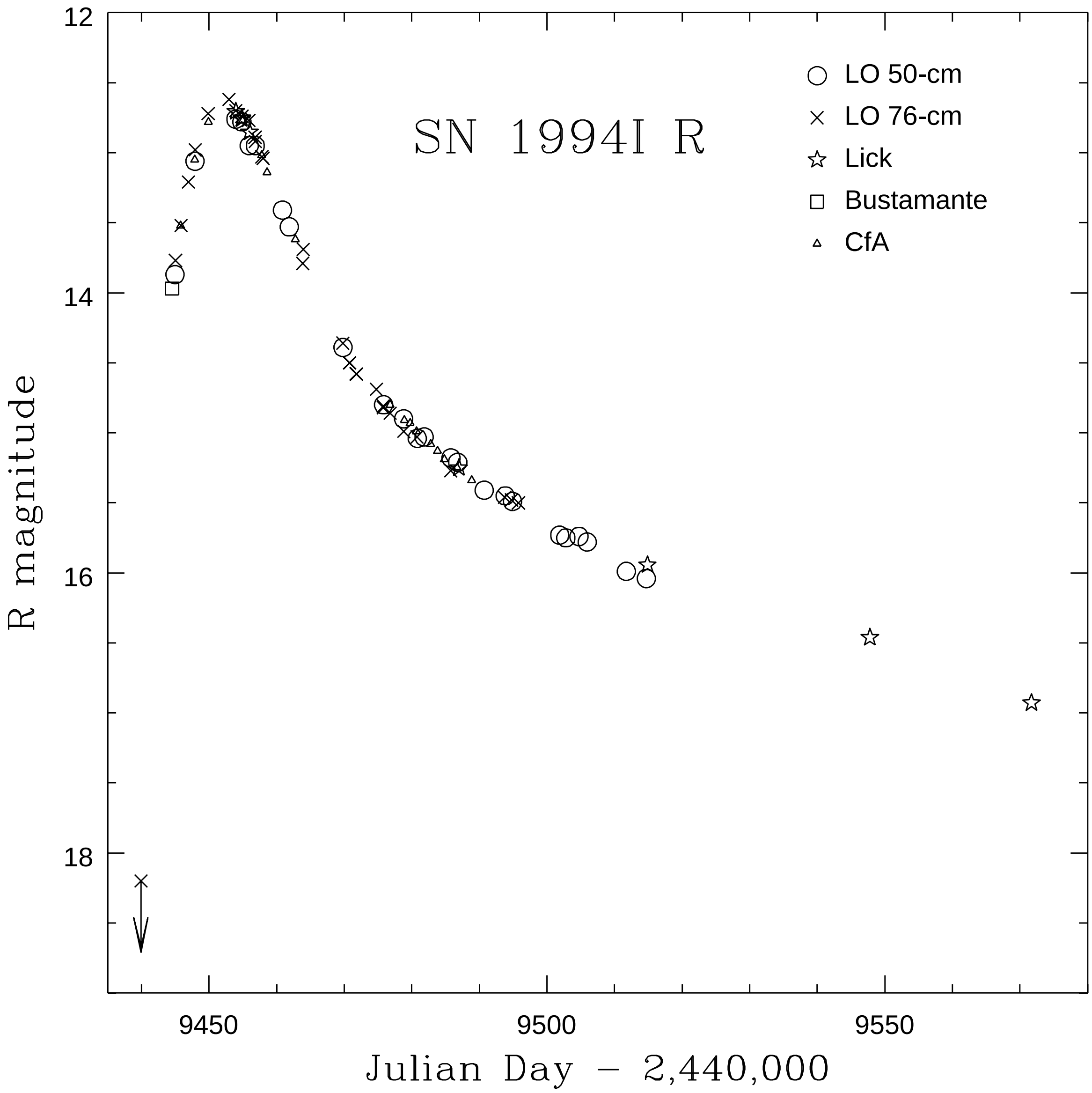

Fig. 8.— *R* light curve of SN 1994I. The data labelled "CfA" were provided by Schmidt & Kirshner (1994b).

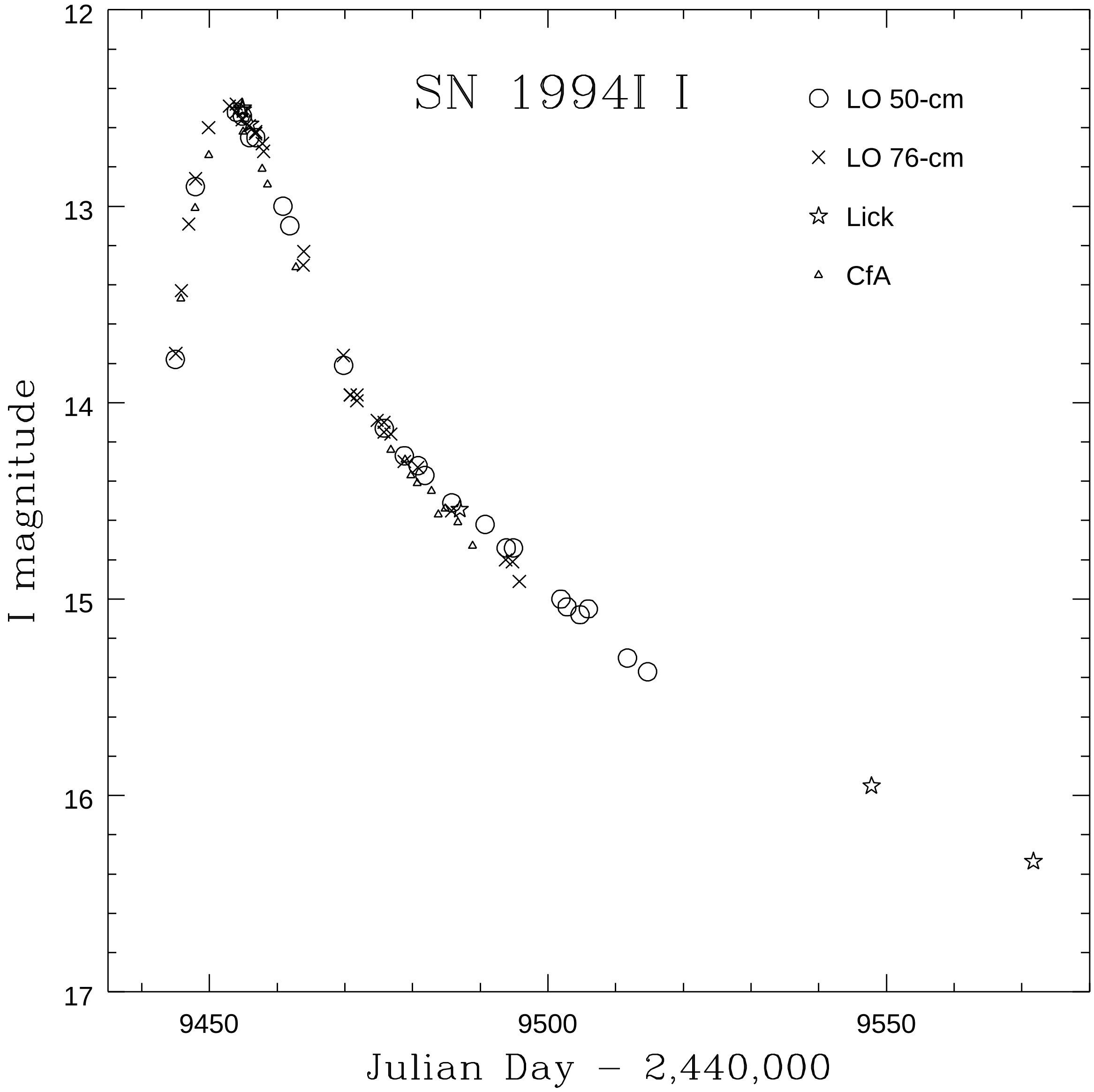

Fig. 9.— *I* light curve of SN 1994I. The data labelled “CfA” were provided by Schmidt & Kirshner (1994b).

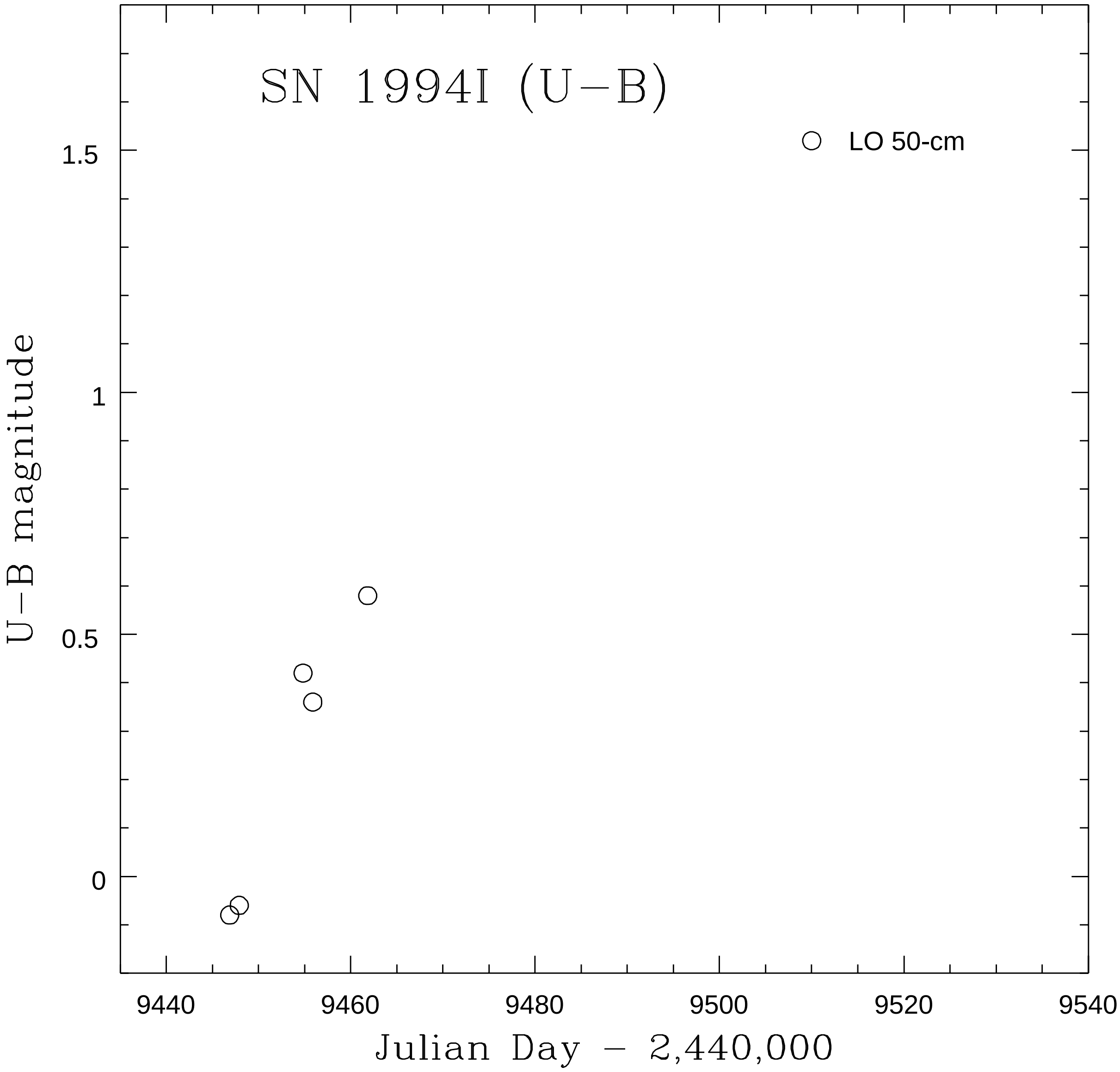

Fig. 10.— $U-B$ color curve of SN 1994I. No reddening corrections have been applied.

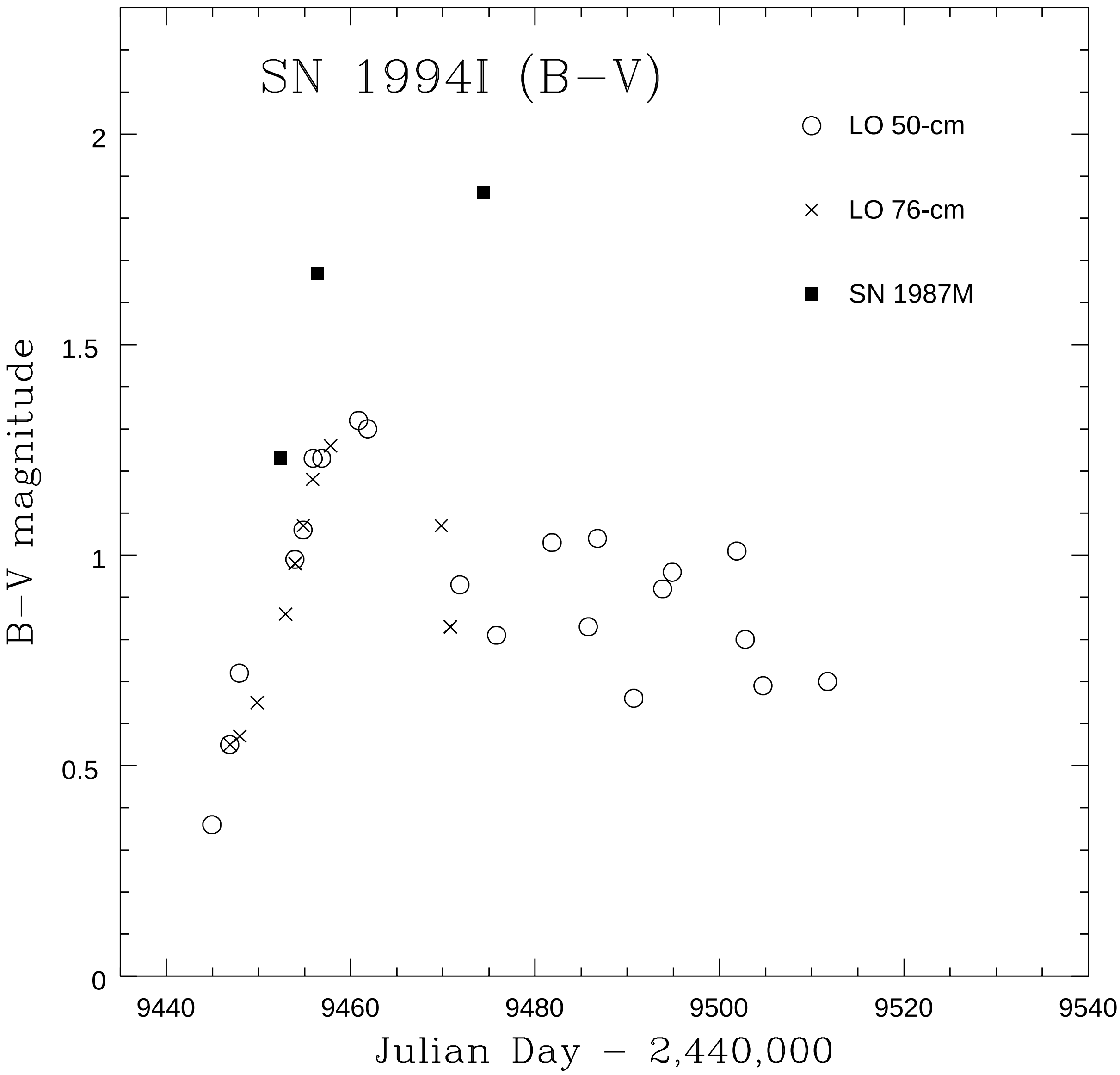

Fig. 11.— $B-V$ color curve of SN 1994I. No reddening corrections have been applied. We also include points for the type Ic SN 1987M, which have been shifted in time slightly (see Section 8).

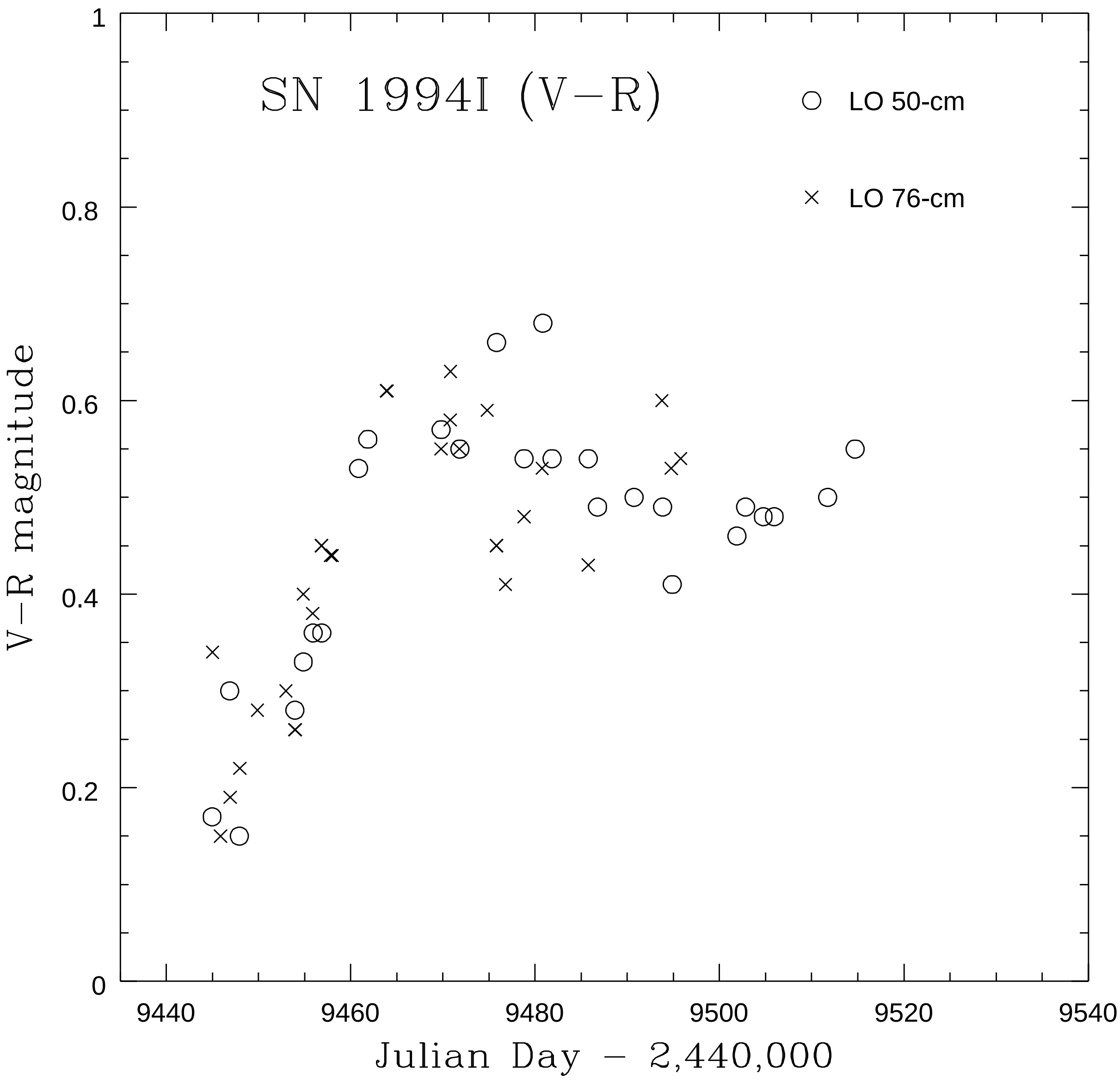

Fig. 12.— $V - R$ color curve of SN 1994I. No reddening corrections have been applied.

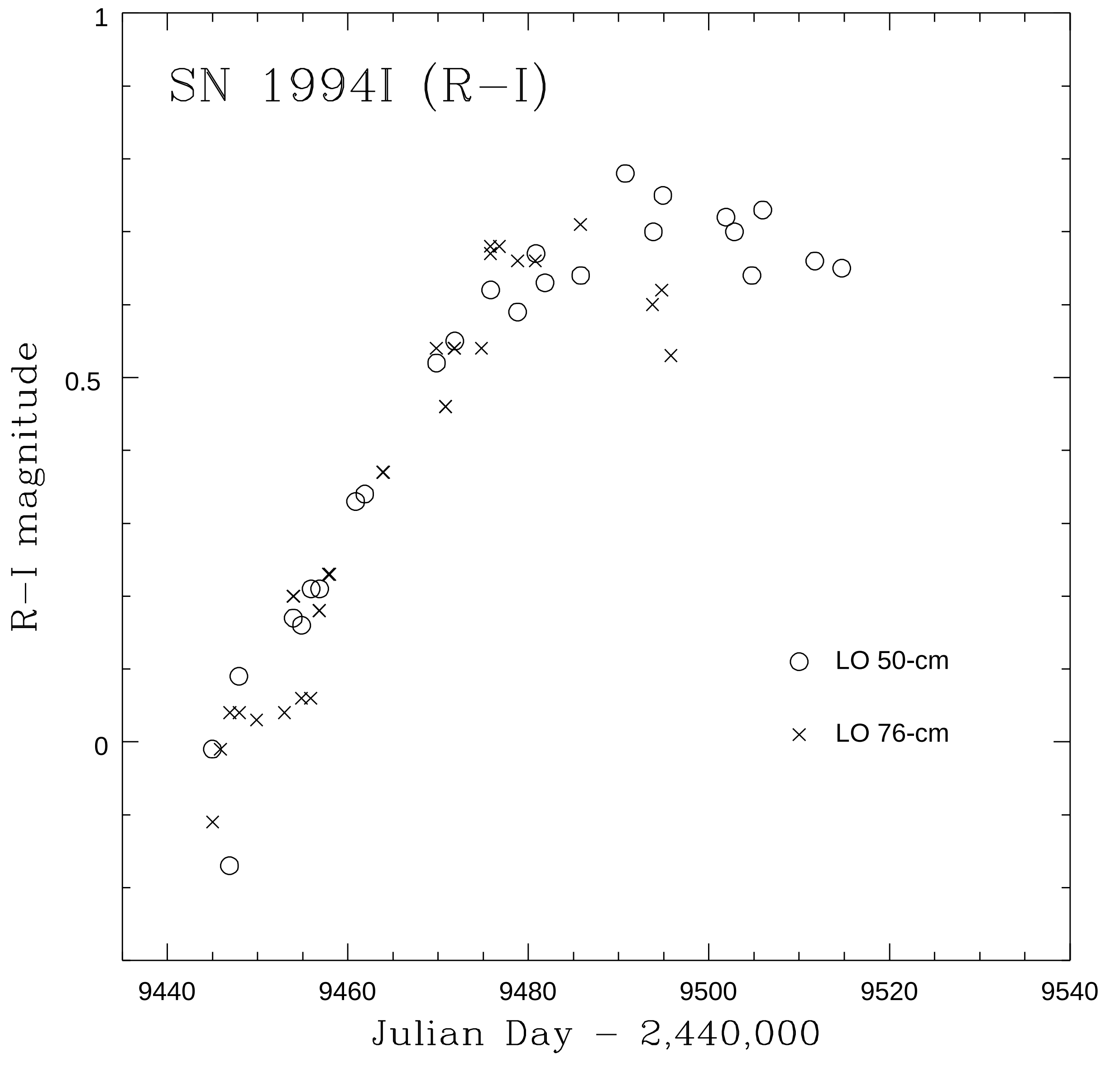

Fig. 13.— $R - I$ color curve of SN 1994I. No reddening corrections have been applied.

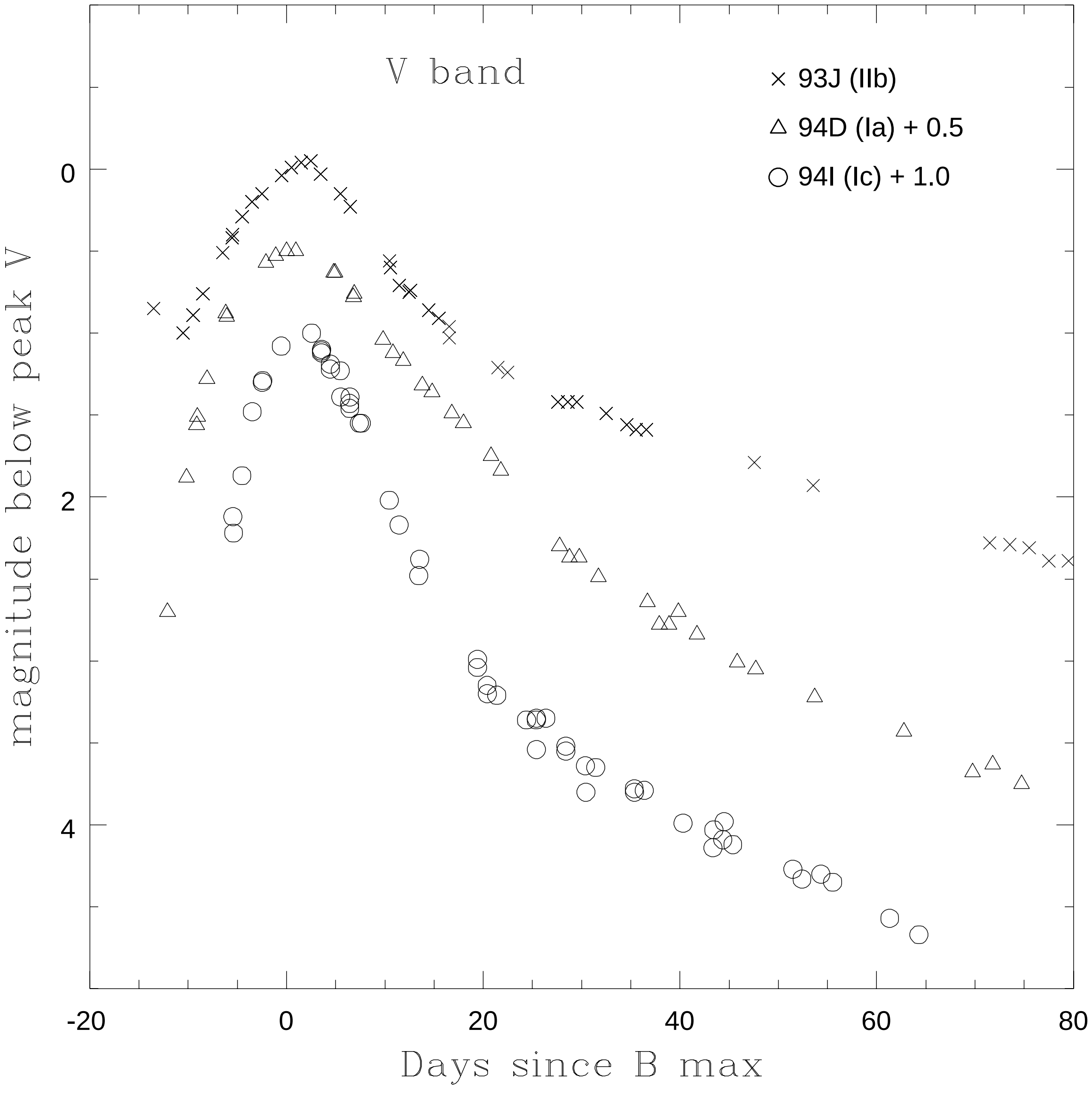

Fig. 14.— Comparison of the V-band light curves of SNe 1994I, 1994D and 1993J.

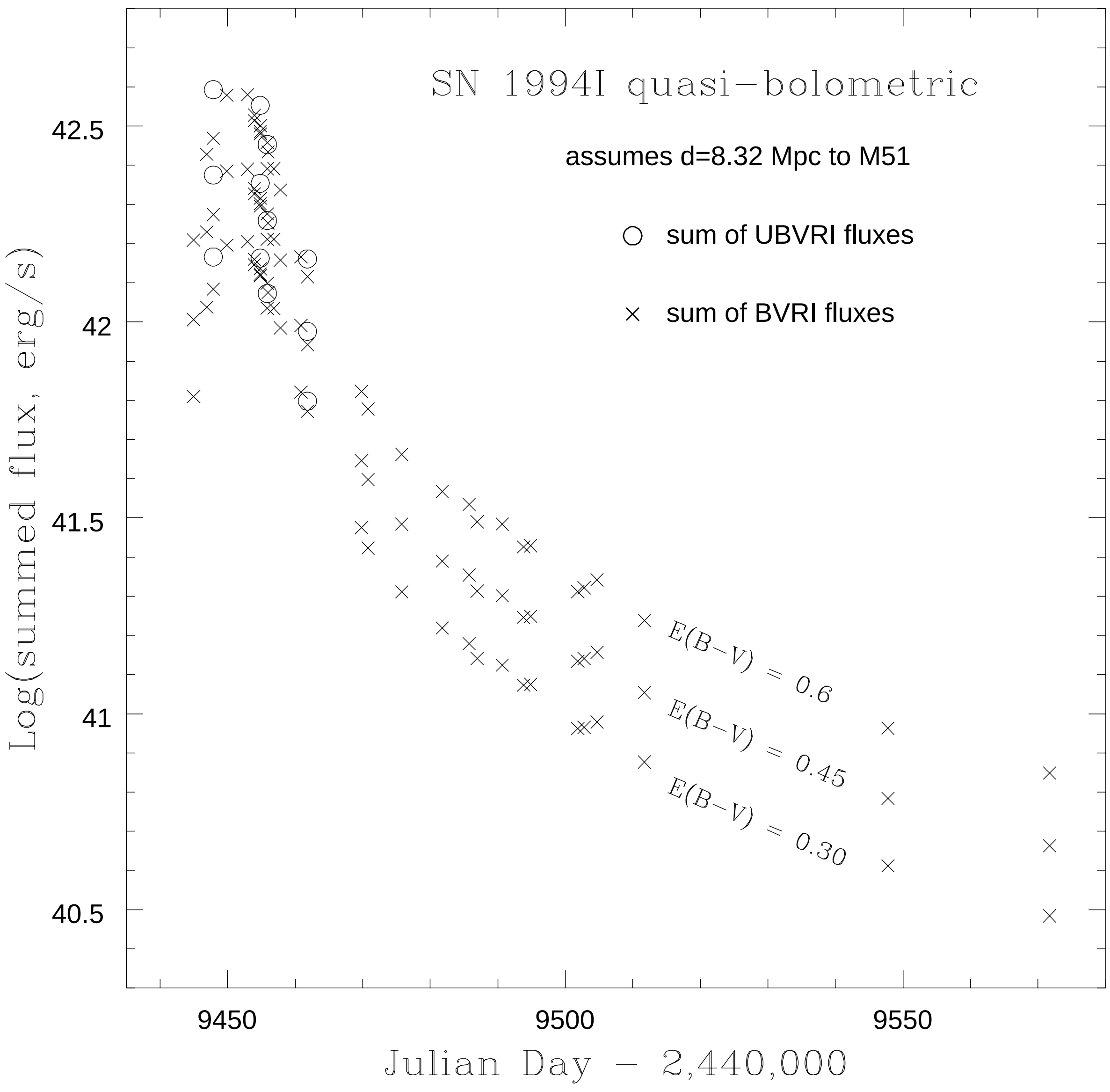

Fig. 15.— Quasi-bolometric light curves, formed by summing optical fluxes. Note the difference between *UBVRI* and *BVRI* sums for high values of color excess.

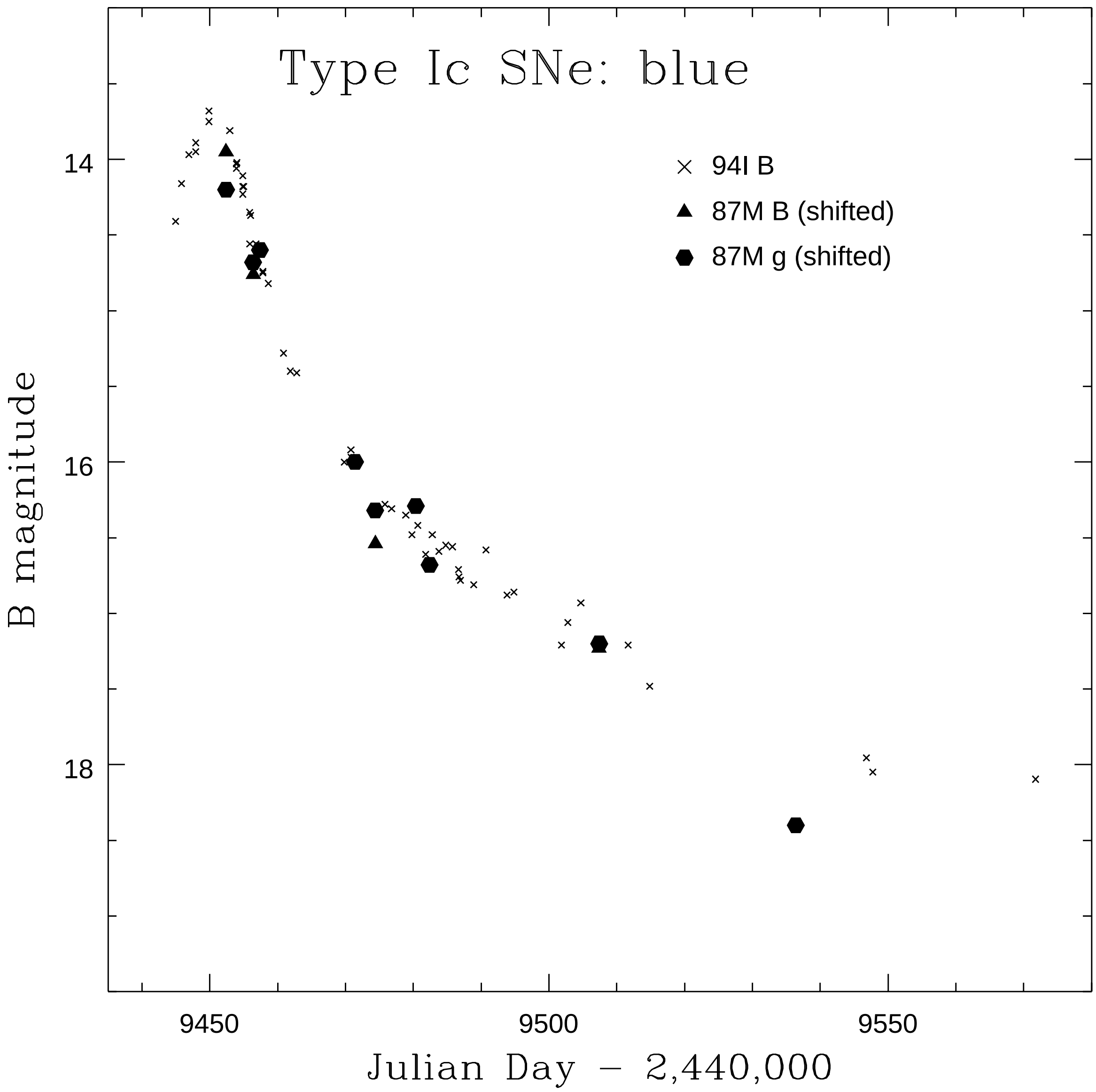

Fig. 16.— Comparison of the type Ic SNe 1994I and 1987M in blue passbands. The data for 1987M have been shifted by (+5 days, -2.3 mag) in B, (+5 days, -1.0 mag) in g.

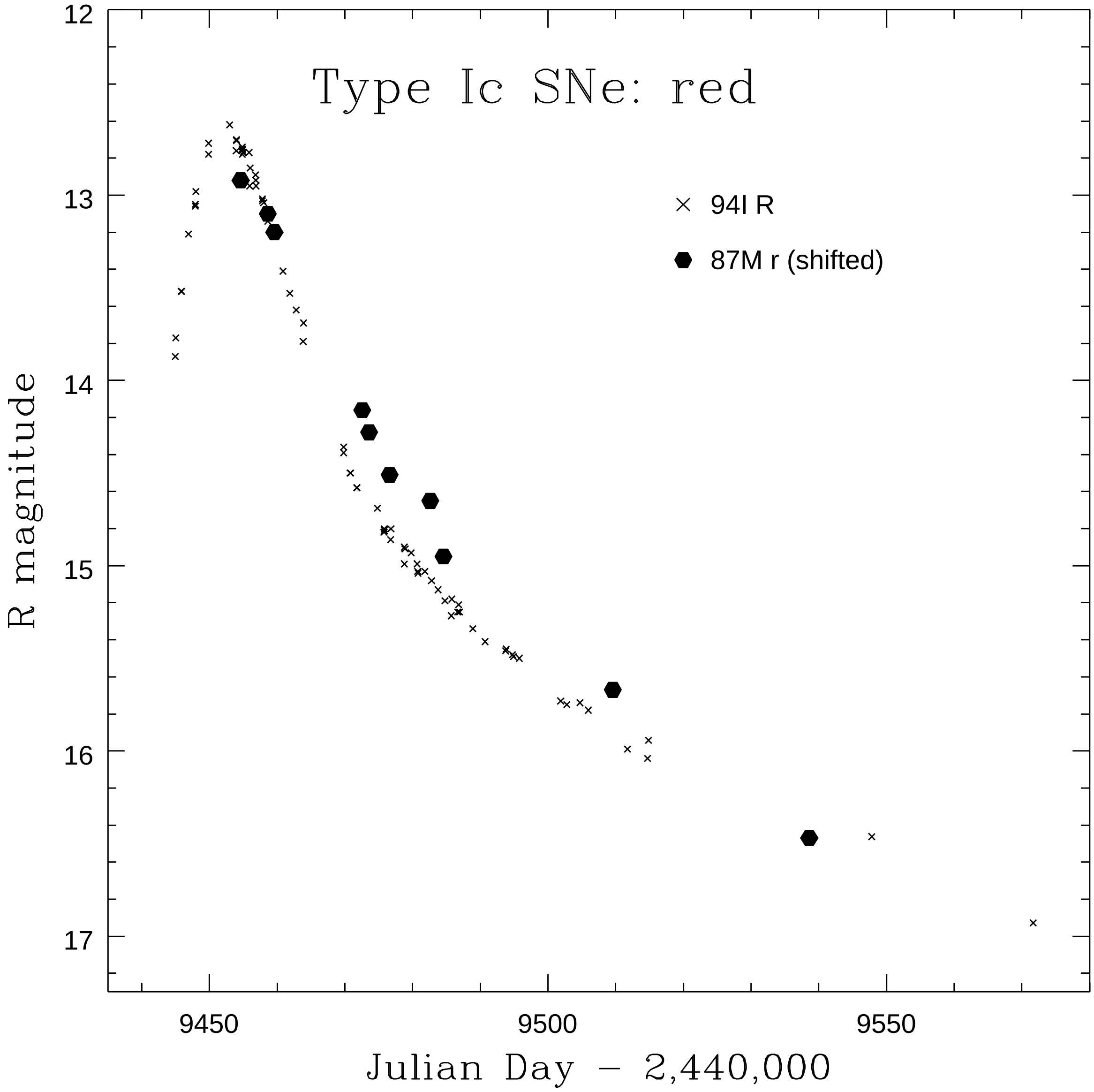

Fig. 17.— Comparison of the type Ic SNe 1994I and 1987M in red passbands. The data for 1987M have been shifted by (+5 days, -2.0 mag) in r.